11-2022

Filling Critical Gaps in the Space-Time Record of High Lava Plains and co-Columbia River Basalt Group rhyolite Volcanism

Vanessa Marie Swenton
Portland State University, vmswenton@gmail.com

Martin J. Streck
Portland State University, streckm@pdx.edu

Daniel P. Miggins
Oregon State University

William C. McIntosh
New Mexico Institute of Mining and Technology

Citation Details

Swenton, V. M., Streck, M. J., Miggins, D. P., & McIntosh, W. C. (2022). Filling critical gaps in the space-time record of High Lava Plains and co-Columbia River Basalt Group rhyolite volcanism. GSA Bulletin.

THE GEOLOGICAL SOCIETY OF AMERICA®

Filling critical gaps in the space-time record of High Lava Plains and co-Columbia River Basalt Group rhyolite volcanism

Vanessa M. Swenton[1,†], Martin J. Streck[1], Daniel P. Miggins[2], and William C. McIntosh[3]
[1]*Department of Geology, Portland State University, P.O. Box 751, Portland, Oregon 97207-0751, USA*
[2]*College of Earth, Ocean, and Atmospheric Sciences, Oregon State University, Corvallis, Oregon 97331-5503, USA*
[3]*New Mexico Institute of Mining and Technology, Socorro, New Mexico 87801, USA*

ABSTRACT

Miocene rhyolitic volcanism of eastern Oregon, USA, can be divided into two main episodes. Mantle plume upwelling is thought to have generated Columbia River Basalt Group (CRBG) lavas and coeval >16.5–15 Ma silicic volcanism trending north–south from northeast Oregon to northern Nevada. Rhyolite volcanism of the 12–0 Ma High Lava Plains province has been ascribed to either buoyancy-driven westward plume spreading or to slab rollback and mantle convection spanning from southeast Oregon to Newberry Volcano to the west. The apparent ca. 15–12 Ma eruptive hiatus suggests that rhyolites of these provinces were a product of separate processes, yet this gap was based on incomplete data. The lack of data on ~33 of the total ~50 rhyolitic eruptive centers in the area where the two provinces overlap (117–119°W, 43–44°N) yields only tenuous relationships between these two provinces.

We acquired $^{40}Ar/^{39}Ar$ ages for 29 previously unanalyzed rhyolite centers that confirm the existence of a rhyolitic eruptive episode concurrent with CRBG flood basalt volcanism. Rhyolite eruptions gradually initiated at ca. 17.5 Ma, and our new ages indicate that peak intensity of the first eruptive episode occurred between 16.3 Ma and 14.4 Ma. We refine the ca. 15–12 Ma rhyolitic eruptive hiatus to 14.4–12.1 Ma, where strong recommencement of rhyolite eruptions began with Beatys Butte at 12.05 Ma. We find two prominent fluxes in rhyolitic eruptive activity after 12.1 Ma as opposed to one continuous, age-progressive trend, at 12.1–9.6 Ma and 7.7–5.1 Ma, which are separated by an ~2 m.y. period of decreased rhyolite volcanism. Rhyolite eruptions were scarce after 5.1 Ma, at which point most eruptions were associated with Newberry Volcano. Periodicity of rhyolite volcanism along the High Lava Plains demands more punctuated basalt inputs than what continuous partial melting from west-spreading plume material should generate.

Our new data suggest that regional rhyolite eruptions are a series of episodic events related to the arrival and storage of mafic mantle magmas. Paucity in rhyolite eruptions from 14.4 Ma to 12.1 Ma is related to decreased flux of CRBG flood basalt magmas at ca. 15 Ma. Strong recommencement of rhyolite volcanism at 12.1 Ma is related to continued Northwest Basin and Range extension and a peak rotation rate of Siletzia affecting regional lithosphere weakened by CRBG volcanism. Waning rhyolitic eruptive activity from ca. 9.6 Ma to 7.7 Ma reflects a regional transition in the primary mode of accommodation of extension from Northwest Basin and Range normal faulting to extension and shearing of the Brothers Fault Zone. Rhyolite volcanism between 7.7 Ma and 5.1 Ma was driven by continued regional extension in an area less affected by CRBG magmatism. Post-5.1 Ma rhyolite eruptions occurred within crust not influenced by CRBG magmatism but impacted by both regional extension and the Cascadia subduction zone.

INTRODUCTION

Globally, the vast majority of voluminous outpouring of continental flood basalts is accompanied by coeval silicic volcanism (e.g., Chiesa et al., 1989; Bryan et al., 2002; Tian et al., 2010). Numerous workers have studied the basalts of these bimodal provinces, but significantly less work has focused on the silicic volcanism. Recently, greater focus has been placed on understanding the silicic member of bimodal provinces, because it has become increasingly apparent that these silicic volcanic deposits provide insight into the storage duration and location of the associated basaltic magma and into the complexities of the magmatic and tectonic systems involved (e.g., Streck et al., 2015, 2017; Webb et al., 2019; Arakawa et al., 2019).

The Columbia River Basalt Group (CRBG) of the Pacific Northwest, USA, the world's youngest flood basalt province, is one of these bimodal systems (Fig. 1). Voluminous outpourings of mostly mid-Miocene basalts of the CRBG and late Miocene basalts of the High Lava Plains (HLP) volcanic provinces in eastern Oregon were accompanied by silicic volcanism that manifested as coeval caldera complexes and dome fields. The less studied ca. 16.5–0 Ma rhyolite ash-flow tuffs, lava flows, and domes of these expansive, bimodal systems are of complex origin. Older, ca. 16.5–15 Ma rhyolites coeval with the CRBG eruptions are widely accepted as being associated with the Yellowstone mantle plume (e.g., Camp et al., 2003; Streck et al., 2015). However, some studies propose that upper mantle and tectonic processes are involved in the generation of CRBG flood basalts rather than a deep-sourced mantle plume (e.g., Christiansen et al., 2002; Leeman and Streck, 2021). Younger, 12–0 Ma rhyolites are generally associated with the northwest-younging HLP trend, where the oldest rhyolitic eruptive centers are located in southeast Oregon and the youngest rhyolites are found around Newberry Volcano near the Cascades volcanic arc.

The co-CRBG and HLP rhyolite provinces were interpreted as separate and distinct due to (1) lack of regional silicic centers between the youngest co-CRBG (ca. 15 Ma) and the oldest associated with the HLP (ca. 12 Ma) and (2) the perception that almost no co-CRBG rhyolites have been emplaced farther west than ~118°W. However, sparse, recently acquired age data indicate that rhyolites as far west as 120°W possess ages >15 Ma (e.g., Webb et al., 2019; Fig. 1). These newer data imply that the two provinces overlap spatially. Numerous silicic centers within the primary area of spatial overlap remained undated, and few had been geochemically analyzed (Fig. 2).

[†]vswenton@pdx.edu.

GSA Bulletin;
published online 23 September 2022

https://doi.org/10.1130/B36346.1; 9 figures; 3 tables; 1 supplemental file.

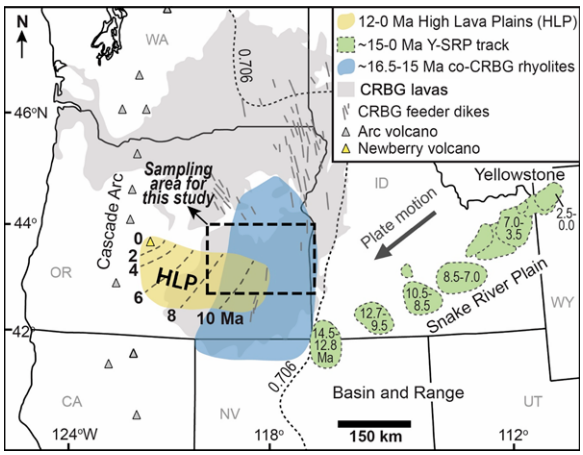

Figure 1. Map shows primary regional Miocene volcanic provinces, modified from Coble and Mahood (2012, 2016) and Camp (2019). Extent of co-Columbia River Basalt (co-CRBG) rhyolites reflects new ages from recent studies (e.g., Streck et al., 2015; Sales, 2018; Webb et al. 2019). The fine, dashed line is a 0.706 Sr isotope line that represents the approximate craton boundary. Age ranges for the Yellowstone–Snake River Plain (Y-SRP) calderas are from Perkins and Nash (2002). HLP—High Lava Plains.

Current studies pose varying models of the magmatic and tectonic processes responsible for generating HLP rhyolites. The motivation for these studies lies in addressing the peculiarity of the northwest-younging HLP rhyolite volcanic trend that mirrors the adjacent northeast-younging Yellowstone–Snake River Plain (YSRP) trend (Fig. 1). In deep-sourced mantle plume models, the YSRP trend is interpreted as an expression of the Yellowstone plume tail that is currently active at Yellowstone caldera (e.g., Pierce and Morgan, 1992). Recent studies suggest that HLP rhyolites correlate either to (1) the Yellowstone mantle plume similar to co-CRBG rhyolites (Jordan et al., 2004; Camp and Ross, 2004; Camp, 2019; Camp and Wells, 2021) or (2) slab rollback and mantle convection related to the subducting Cascadia slab beneath the North American plate (Long et al., 2009; Chen et al., 2013; Ford et al., 2013; Till et al., 2013). Some also incorporate fragmentation or tearing of the slab (Zhou et al., 2018; Hawley and Allen, 2019). Our study compiles new and earlier geochronological data to fill gaps in the space-time distribution of regional rhyolites. We use these data to evaluate previous models and construct a new model for HLP rhyolite volcanism and to analyze its relationship to co-CRBG rhyolite volcanism.

This study highlights the complex magmatic and tectonic phenomena involved in continental flood basalts and bimodal volcanic systems. This work also underscores the dependence of basalt input associated with mantle upwelling

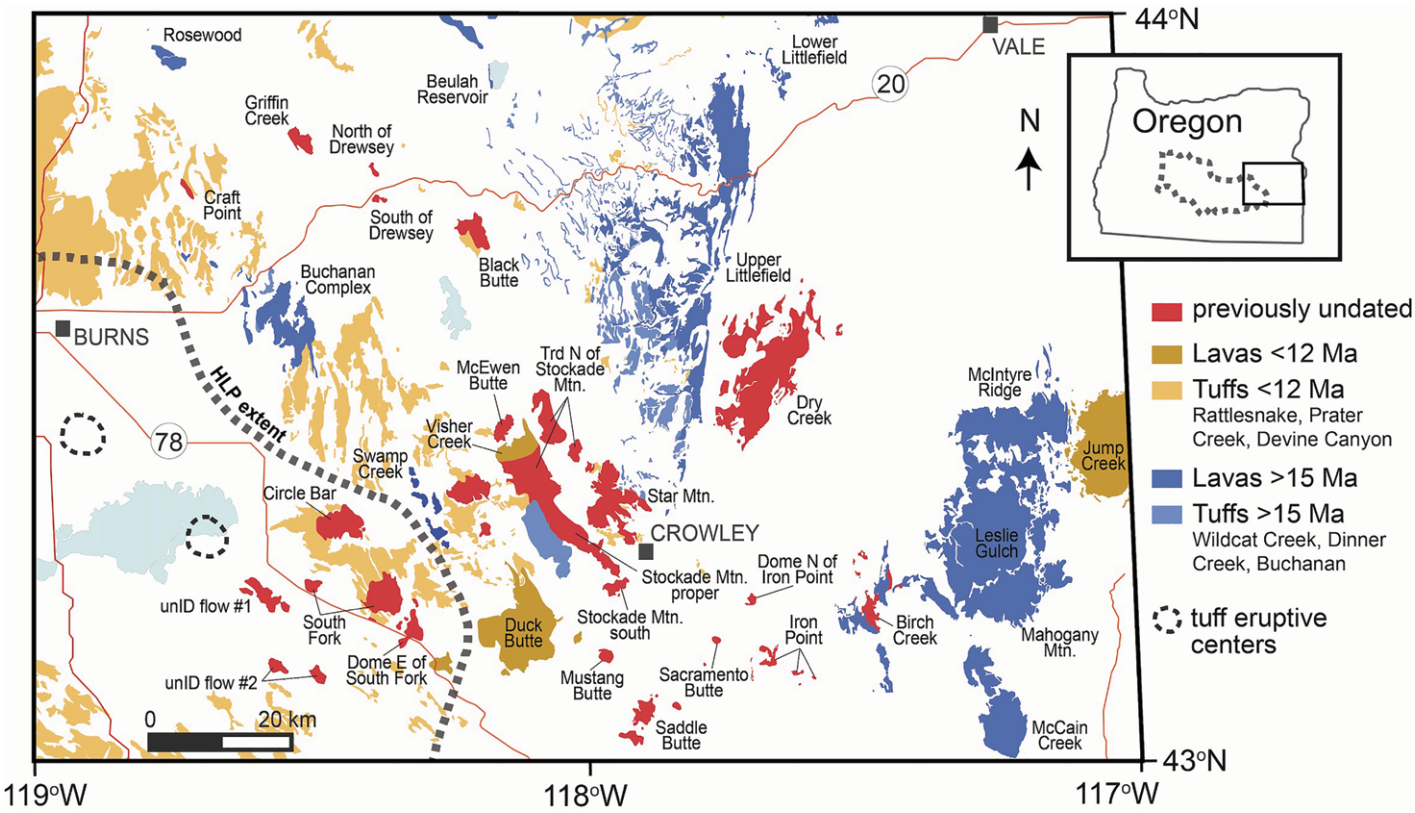

Figure 2. Compilation geologic map shows Miocene silicic centers in the primary sampling area of this study (outlined in Fig. 1) and highlights silicic units of the co-Columbia River Basalt Group (>15 Ma; shades of blue), High Lava Plains (HLP; <12 Ma; shades of yellow), and the abundance of missing ages for centers in the area where the two provinces overlap. Red color denotes a center that was undated or had yet to be precisely dated (only a K-Ar or stratigraphic age is reported). HLP extent and Devine Canyon and Prater Creek Tuff eruptive centers are from Ford et al. (2013). Leslie Gulch, Mahogany Mountain, and McIntyre Ridge areas include all units associated with the Mahogany–Three Fingers rhyolite field. Sources for ages are in Supplemental Material A.1 (see text footnote 1). E—East; N—North; Trd—Unit abbreviation from Greene et al. (1972) for undifferentiated Miocene "Rhyodacite"; unID—unidentified.

on rhyolite volcanism, where upwelling mantle may include a deep-sourced Yellowstone mantle plume during the early phase of rhyolite volcanism. Our interpretations highlight the relationship between faulting and magma storage that can be applied to other global bimodal systems, particularly those influenced by multiple tectonic regimes.

EARLIER RHYOLITE GEOCHRONOLOGY

About 50 rhyolitic eruptive centers lie exposed in the area where co-CRBG and HLP rhyolite provinces overlap (117–119°W, 43–44°N; Fig. 2). Here, a distinct silicic center is defined by a mapped area of silicic volcanic rock that (1) is confirmed as a silicic eruptive center through previous work or which mapped topographic relief indicates is an eruptive center, (2) possesses a geochemical signature distinct from that of other nearby centers, and/or (3) is of an age beyond error of that of adjacent centers. Of the ~50 centers, ~17 had been dated and ~33 were undated.

Previously determined ages of silicic centers throughout eastern Oregon fall almost exclusively within ca. 16.5–15.0 Ma and ca. 12.0–0 Ma (Supplemental Material A.1[1]). Rhyolites of Bald Butte (17.5 Ma; Jordan et al., 2004), Drum Hill (17.3 Ma; Jordan et al., 2004), Unity (17.0–16.5 Ma; Streck et al., 2017), and the Strawberry Volcanics (ca. 16.2–14.7 Ma; Steiner and Streck, 2018) were the only known exceptions outside of those two age ranges. This lack of ages between ca. 15 Ma and 12 Ma implied the potential existence of an ~3 m.y. regional rhyolitic eruptive hiatus, but this remained uncertain without precise ages for all silicic centers.

Although Benson and Mahood (2016) suggest a northward-younging progression in co-CRBG silicic volcanism, there is little evidence for a space-time trend (Streck et al., 2017). In contrast, silicic volcanism of the HLP province displays a definitive northwest-younging age progression (e.g., Walker, 1974; MacLeod et al., 1976; McKee and Walker, 1976; Jordan et al., 2004; Ford et al., 2013) that parallels the northwest-trending Brothers Fault Zone (Jordan, 2002, 2004). Before our study, the oldest dated rhyolite centers associated with the HLP included Visher Creek (11.0 Ma; K-Ar age from Walker, 1979) and Duck Butte (10.5 Ma; Johnson and Grunder, 2000). The younging trend culminates at Newberry Volcano with rhyolites as young as the 1.3 ka Big Obsidian Flow (radiocarbon age from Robinson and Trimble, 1983).

REGIONAL BIMODAL VOLCANISM

Columbia River Basalt Group and Yellowstone–Snake River Plain Provinces

Numerous studies posit that the ca. 17.2–15.6 Ma flood basalts and basaltic andesites of the CRBG are the result of a rising deep-sourced mantle plume impinging on the base of the North American lithosphere (e.g., Morgan, 1981; Griffiths and Campbell, 1991; Weinberg, 1997; Camp and Ross, 2004; Coble and Mahood, 2012). Other recent studies associate the plume's origin with the Siletzia province, where initial plume-lithosphere interactions began much earlier, at ca. 42–34 Ma, and continued to present day as the North American plate migrates over the plume tail (e.g., Wells et al., 2014; Camp and Wells, 2021). In either case, hotter mantle ponded at the base of the lithosphere roughly along the west side of the craton boundary (Fig. 1), where basaltic magma then propagated to the surface via dikes and erupted as the initial CRBG basalts (e.g., Hooper et al., 2002). Conversely, some studies have argued that CRBG flood basalt geochemical signatures more closely resemble melting of subcontinental lithosphere via Basin and Range extension than they resemble a deep-sourced mantle plume (e.g., Leeman and Streck, 2021). Such studies have related the Yellowstone system to processes such as upper mantle convection and regional tectonics (e.g., Christiansen et al., 2002).

Either fractional crystallization or partial melting of continental crust resulted in the coeval ca. 16.5–15 Ma silicic volcanism (e.g., Camp et al., 2003). Rhyolitic eruptive centers associated with this period include those of the Three Fingers–Mahogany Mountain, McDermitt, Santa Rosa–Calico, and High Rock caldera complexes (e.g., Brueseke and Hart, 2008; Shervais and Hanan, 2008; Coble and Mahood, 2012; 2016), as well as the Dinner Creek Tuff, Littlefield, Dooley Mountain, Wildcat Creek Tuff, Buchanan, and Strawberry rhyolites and a number of other smaller rhyolite centers farther north (e.g., Steiner and Streck, 2013; Streck et al., 2015, 2017; Webb et al., 2019; Fig. 2). Previous work on co-CRBG rhyolites in the study area (Fig. 2) indicates that rhyolites range from ~70–77 wt% SiO_2, 0.7–6.0 wt% FeO*, and 11–15 wt% Al_2O_3 (Fig. 3).

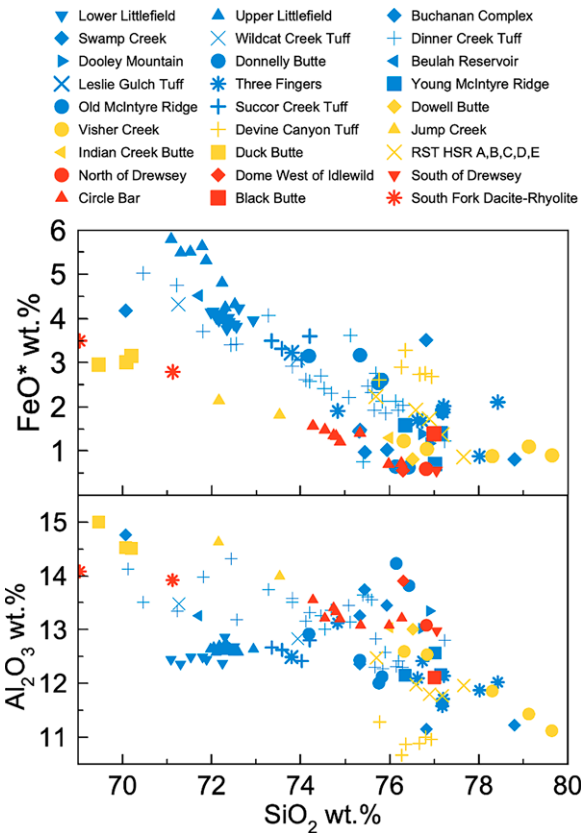

Figure 3. Compilation of compositional data of regional Miocene rhyolite centers from previous studies highlights the significant variation among >15 Ma co-CRBG (blue) and <12 Ma High Lava Plains (HLP; yellow) centers and the abundance of centers that are yet to be dated (red). All centers included are lavas unless otherwise noted in the legend. RST HSR—Rattlesnake Tuff high-silica rhyolites. See Supplemental Material B (see text footnote 1) for sources.

[1]Supplemental Material. (A) Referenced ages and sample locations; (B) Sources of pre-existing geochemical data; (C) $^{40}Ar/^{39}Ar$ ideograms and plateaus; (D) Detailed $^{40}Ar/^{39}Ar$ analysis sample preparation procedures and analytical methods; (E) Full argon data files—feldspar and groundmass analyzed at OSU; and (F) Full argon data files—biotite analyzed at OSU. Please visit https://doi.org/10.1130/GSAB.S.20394384 to access the Supplemental Material, and contact editing@geosociety.org with any questions.

TABLE 1. PREVIOUSLY REPORTED $^{40}AR/^{39}AR$ AGES FOR 15–10 MA REGIONAL BASALTIC ERUPTIONS

Formation association	Unit dated*	Age (Ma)	Error (±2σ) (m.y.)	Source
Keeney Sequence		10.1	1.4	Hooper et al. (2002)
Keeney Sequence	Riverside lavas	10.1	0.23	Camp et al. (2003)
Keeney Sequence		10.3	1.2	Hooper et al. (2002)
Keeney Sequence		10.4	0.8	Hooper et al. (2002)
Keeney Sequence		11.5	2	Hooper et al. (2002)
Keeney Sequence		11.5	0.4	Hooper et al. (2002)
Keeney Sequence		12.2	0.2	Hooper et al. (2002) cites Dunnean (1998)
Keeney Sequence	Buck Mountain	12.5	0.05	Camp et al. (2003)†
Tims Peak Basalt	Prava Peak	13.1	0.2	Hooper et al. (2002) cites Dunnean (1998)
Tims Peak Basalt	Hat Top	13.4	3.6	Hooper et al. (2002)
Keeney Sequence		13.4	0.8	Hooper et al. (2002)
Tims Peak Basalt	Hat Top	13.6	0.2	Hooper et al. (2002) cites Dunnean (1998)
Tims Peak Basalt		13.8		Wright et al. (2016)
Owyhee Basalt		13.8	0.3	Fiebelkorn et al. (1983)
Tims Peak Basalt	Prava Peak	13.9	0.2	Hooper et al. (2002)
Owyhee Basalt		14.1		Fiebelkorn et al. (1983) cites Laursen and Hammond (1974)
Owyhee Basalt		15	0.3	Fiebelkorn et al. (1983) cites Baksi and Watkins (1973), Watkins and Baksi (1974) and Laursen and Hammond (1974)

Note: This table includes basaltic flows known to have erupted within the study region between 15–10 Ma, and thus it does not include later non-main phase eruptions associated with the Columbia River Basalt Group that erupted outside of the study region.

*Specific unit dated only listed if specified from source.

†Referred to as Buck Mountain of Keeney Sequence because of similarities to Shumway Basalt from Fiebelkorn et al. (1983).

Initiation of the well-defined, northeast age-progressive trend of YSRP silicic volcanism is interpreted as being due to the transition from volcanism as a result of widespread plume material to volcanism as a result of heating by the narrower plume tail as it was overridden by the North American craton (e.g., Draper, 1991; Pierce and Morgan, 1992; Smith and Braille, 1994; Christiansen et al., 2002; Perkins and Nash, 2002; Camp and Ross, 2004, Camp and Wells, 2021). The first rhyolite volcanism associated with the YSRP age-progressive trend were caldera eruptions of the Owyhee Plateau–Bruneau Jarbidge–Twin Falls Volcanic Field, which began at ca. 14 Ma (Pierce and Morgan, 1992; Shervais and Hanan, 2008).

15–12 Ma: A Shift in Regional Mafic Magmatism Related to Mantle Dynamics

In the deep-sourced plume model of CRBG volcanism, the rate of ponding and radial spreading of plume material at the craton boundary (Fig. 1) waned at ca. 15 Ma, when the plume was overridden by the west-migrating craton (Draper, 1991; Pierce and Morgan, 1992; Parsons et al., 1994; Camp et al., 2003; Camp and Ross, 2004). Post-15 Ma, the plume head migrated westward at ~53 km/Ma (Ford et al., 2013), likely aided by Cascadia slab subduction-induced counterflow (Draper, 1991; Pierce et al., 2000; Camp and Ross, 2004; Ford et al., 2013; Wells and McCaffrey, 2013; Camp, 2019).

After late eruptions of tholeiitic CRBG flood basalts, such as the 16.0–16.1 Ma Hunter Creek Basalt (Webb et al., 2019), there was a notable transition in the composition of mafic eruptions in eastern Oregon. From ca. 15.0–10.1 Ma, voluminous eruptions of high-alumina olivine tholeiites (HAOTs) and calc-alkaline to mildly alkaline mafic to intermediate lavas were emplaced throughout eastern Oregon, including the ca. 15.0–13.1 Ma Owyhee Basalt, the ca. 13.9–13.1 Ma Tims Peak Basalt, and the ca. 13.5–10.1 Ma Keeney Sequence (Table 1). Lavas of the Tims Peak Basalt are considered the oldest known HAOTs (Ferns et al., 1993a; Hooper et al., 2002; Camp et al., 2003), but the oldest HAOTs recognized in the area where co-CRBG and HLP rhyolites spatially overlap are 11.0–8.0 Ma (Camp and Ross, 2004).

HAOTs with depleted mantle, MORB-like source signatures reflect decompression melting of upper lithospheric mantle (e.g., Carlson and Hart, 1988; Hooper and Hawkesworth, 1993; Conrey et al., 1997) as is also suggested by experimental studies indicating equilibrium at shallow mantle pressures (Bartels et al., 1991; Till et al., 2013). Thus, the westward-younging episodes of HAOT volcanism from easternmost Oregon toward the Cascade volcanic arc and Newberry Volcano (Hart et al., 1984; Christiansen et al., 2002) are interpreted as reflecting the westward spread of hot plume material (Camp and Ross, 2004; Jordan et al., 2004). The progressive westward decline in radiogenic mantle signatures of HAOTs has been attributed to a progressive decrease in the influence of Yellowstone mantle, lithospheric mantle, or both (e.g., Carlson and Hart, 1987; Camp and Ross, 2004).

These broad variations in mafic magma compositions correspond with coeval tectonic activity. Workers have provided evidence for regional uplift as a crustal response to the ponding of hotter mantle (plume?) material (Lowrey et al., 2000; Glen and Ponce, 2002; Camp, 2019), where extension led to crustal weaknesses that allowed CRBG flood basalt magmas to reach the surface via dikes (e.g., Camp, 1995; Pierce et al., 2000; Camp and Ross, 2004). This regional uplifting peaked at ca. 15 Ma (Pierce et al., 2000) and coincided with the migration of the North American plate over the plume tail. Significant localized extension in eastern Oregon initiated with the formation of the Oregon-Idaho graben at ca. 16 Ma (Webb et al., 2019). Intragraben normal faulting at ca. 14.3–12.6 Ma accompanied mafic to intermediate calc-alkalic volcanism (Cummings et al., 2000). It is postulated that large, regional fault systems like the Brothers Fault Zone may have allowed the younger HAOT magmas to reach the surface via dikes (Christiansen et al., 2002; Camp and Ross, 2004; Jordan et al., 2004).

Post-12 Ma: High Lava Plains Province

The bimodal HLP province is characterized broadly by an abundance of HAOTs and basaltic andesitic flows, crystal-poor rhyolites, and sparse intermediates (e.g., Jordan et al., 2004; Streck and Grunder, 2008, 2012; Ford et al., 2013). HLP mafic volcanism <8 Ma is a product of prolonged differentiation of primitive HAOTs and crustal contamination (Streck and Grunder, 2012). Most HLP rhyolites are described as high-silica and aphyric to sparsely phyric, with less common lower silica rhyolites (Linneman and Myers, 1990; MacLean, 1994; Streck and Grunder, 1997; Johnson and Grunder, 2000; Streck and Grunder, 2008). Previous work on HLP rhyolites in the study area (Fig. 2) indicates that rhyolites range from ~69.5 wt% to 77 wt% SiO_2, ~0.8–3.3 wt% FeO*, and ~11–15 wt% Al_2O_3 (Fig. 3). Trace element variations among HLP high-silica rhyolites are extraordinary (cf. Streck and Grunder, 2008; Hess, 2014).

The magmatic and tectonic processes responsible for generating HLP rhyolites remain unclear. Involvement of the Yellowstone mantle plume in rhyolite volcanism of the HLP has been proven difficult to explain, because the age-progression mirrors that of the YSRP trend. Here we present the most recently proposed models.

Several models incorporate the Yellowstone mantle plume in their explanation of the northwest-younging trend in HLP silicic volcanism. Jordan et al. (2004) proposed that post-17 Ma, the mantle plume head was flowing along basal lithospheric topography, where the plume buoyantly rose from the base of thicker cratonic lithosphere to the east to the base of thinner accreted lithosphere to the west. They explained that a combination of basal lithospheric flow, small-scale convection from mantle and

relatively hotter plume interaction, and subduction-induced counterflow caused the northwest migration of the resulting rhyolite volcanism in the HLP. Camp (2019) compiled seismic, geochemical, isotopic, geochronological, and geophysical data to conclude that the HLP trend is a result of channelized lateral flow of plume-modified mantle interacting with the lithosphere, where the mantle buoyantly spreads "uphill" and around thicker continental lithosphere anomalies. Camp and Wells (2021) built upon the models proposed by Jordan et al. (2004) and Camp (2019), but instead of initial westward buoyancy-driven plume spreading occurring when the plume tail was beneath the craton boundary, they propose this occurred when the tail was already well established beneath the YSRP track.

Alternative models attribute the HLP silicic volcanic trend to mechanisms related to the Cascadia slab and do not involve the plume. Ford et al. (2013) proposed a model where Cascadia slab rollback, trench migration due to westward advancement of the North American plate, and continuous steepening of the slab caused strong toroidal flow of the mantle focused under the HLP. These processes, along with asymmetrical slab rollback, resulted in greater amounts of extension in southern Oregon than in central–northern Oregon, basaltic magma propagation via dikes, and subsequent crustal melting that produced the HLP trend (Ford et al., 2013). They dated rhyolites in northern Nevada and far southeast Oregon, extending the age progression of the HLP trend to include rhyolites in the northernmost Basin and Range province. Wells and McCaffrey (2013) described mantle counterflow at the rate of slab subduction as the mechanism driving HLP age-progressive volcanism. Hawley and Allen (2019) compiled petrologic, geologic, marine geophysical, and seismic data from numerous studies to propose that the HLP trend results from a westward, up-dip propagating tear in the late Juan de Fuca slab that acts as a hole through which the mantle could flow and interact with the overriding crust.

ANALYTICAL METHODS

Fresh or minimally altered samples were collected from silicic units within the study region that were known to be undated or imprecisely dated. Samples with the greatest abundance of fresh feldspar phenocrysts were the primary targets for $^{40}Ar/^{39}Ar$ dating. Thin sections were prepared by Spectrum Petrographics in Vancouver, Washington, USA. Thin sections from one or two samples of each eruptive center were petrographically analyzed to determine which had suitable feldspars and to identify the best candidates for $^{40}Ar/^{39}Ar$ analysis. A series of mineral separation techniques was implemented to isolate clean feldspar phenocrysts from each sample, including but not limited to magnetic separation, HF acid leaching, and heavy liquid separation. Groundmass fractions were similarly cleaned, separated, and analyzed if feldspar phenocrysts were too altered or too sparse for analysis. Biotite phenocrysts were also analyzed for any samples that lacked fresh feldspars. Single crystal total fusion was the preferred method for dating feldspar phenocrysts, and incremental heating was preferred for groundmass. Supplemental Material D (see footnote 1 for all Supplemental Material) contains detailed sample preparation procedures and analytical methods for $^{40}Ar/^{39}Ar$ analysis, and it also notes the institution at which each sample was analyzed.

RESULTS

We acquired 29 $^{40}Ar/^{39}Ar$ ages from feldspar and groundmass separates (Table 2, Supplemental Material C; see footnote 1 for all Supplemental Material) and three new $^{40}Ar/^{39}Ar$ ages from biotite separates for previously unanalyzed rhyolite centers. Full argon data for each feldspar and groundmass sample analyzed at Oregon State University is in Supplemental Material E. Full argon data for biotite analyzed at Oregon State University is in Supplemental Material F. Feldspar ages are preferred for samples where both feldspar and biotite were dated. If two samples from the same unit produced ages within 2σ error, we consider these samples to be from the same eruptive unit rather than two different eruptive centers. This was the case only for the two samples dated from Star Mountain and the two samples dated from Circle Bar (Table 2; Supplemental Material C). Thus, we present ages for 27 distinct, previously undated rhyolitic eruptive centers.

All ages acquired in this study range from 16.81 Ma to 7.46 Ma. All silicic centers lie within the previously observed ca. 16.5–15.0 Ma and ca. 12–0 Ma age ranges except for the newly designated 16.81 ± 0.05 Ma Dome East of South Fork, the 14.78 ± 0.05 Ma rhyolite of Dry Creek, and the 14.94 ± 0.20 Ma Birch Creek rhyolite (Table 2). Centers <12 Ma broadly conform to the northwest-younging age trend of the HLP determined by previous workers.

Our new ages highlight a notable and previously unrecognized abundance of distinct rhyolite centers that erupted between ca. 12.1 Ma and 9.6 Ma, focused primarily within the sampling area for this study near Crowley, Oregon (Fig. 2). A cumulative age distribution

TABLE 2. SUMMARY OF $^{40}Ar/^{39}Ar$ AGES FROM THIS STUDY

Sample ID	Unit	Age type	Material	Age (Ma)	Error ($\pm 2\sigma$)	n/n_t†
EJ-12-19	South of Drewsey#	SCTF	sanidine	8.62	0.03	
EJ-12-21B	Griffin Creek	SCTF	sanidine	9.86	0.02	15/30
MS-13-09	McEwen Butte	SCTF	sanidine	10.717§	0.01	
MS-13-10	Visher Creek	SCTF	sanidine	11.46	0.02	26/30
MS-17-DAM	Dam Rhyolite	SCTF	plagioclase	14.74	0.02	30/30
VS17-001	Stockade Mountain	SCTF	sanidine	11.029§	0.013	
VS17-003	Star Mountain	SCTF	sanidine	10.659§	0.02	
VS17-020	Star Mountain	SCTF	sanidine	10.64	0.02	30/30
VS17-034	Stockade Mountain, south#	SCTF	sanidine	11.41	0.04	29/30
VS17-035	Mustang Butte	IH	groundmass	10.84	0.04	15/32
VS17-043	Saddle Butte	SCTF	sanidine	10.94	0.05	30/30
VS17-045	Iron Point	SCTF	sanidine	11.84	0.06	28/30
VS17-046B	Dome N of Iron Point#	SCTF	sanidine	10.57	0.03	29/30
VS17-054	Unidentified Flow #1#	SCTF	sanidine	10.21	0.03	25/30
VS17-056	South Fork	SCTF	sanidine	10.35	0.05	23/30
VS17-065	Sacramento Butte	SCTF	sanidine	11.85	0.06	29/30
VS19-068	Birch Creek	SCTF	plagioclase	15.52	0.05	29/30
VS19-079	Birch Creek	SCTF	plagioclase	14.94	0.2	29/30
VS19-080	Dome E of South Fork#	IH	groundmass	16.81	0.05	10/30
VS19-085	Circle Bar	SCTF	sanidine	10.52	0.02	27/30
VS19-089	Circle Bar	SCTF	sanidine	10.55	0.03	26/30
VS19-093	Unidentified Flow #2#	SCTF	sanidine	9.7	0.03	30/30
VS19-098	Stockade Mountain, proper#	SCTF	sanidine	11.21	0.03	24/30
VS17-101	Trd N of Stockade Mountain#	SCTF	sanidine	11.08	0.03	30/30
VS17-104	Trd N of Stockade Mountain#	SCTF	sanidine	11.47	0.04	29/30
VS17-106	Black Butte	SCTF	sanidine	11.45	0.02	29/30
VS19-109	North of Drewsey#	SCTF	sanidine	7.49	0.02	27/30
VS19-116	Dry Creek	SCTF	sanidine	14.78	0.03	24/30
VS20-125A	Wagontire Mountain	SCTF	plagioclase	14.79	0.05	25/30

Note: Two samples from Star Mountain were dated, and their ages are within 2σ error. We consider these two ages to be from the one distinct eruptive center. This is also the case for the two samples dated from Circle Bar. See Supplemental Appendix E (see text footnote 1 for all appendices) for full argon data for all feldspar and groundmass separates analyzed at Oregon State University. See Supplemental Appendix F for full argon data for three biotite separates analyzed at Oregon State University.

*IH—Incremental heating; SCTF—Single crystal total fusion; Trd—unit abbreviation from Greene et al. (1972) for undifferentiated Miocene "Rhyodacite."

†n—number of crystals analyzed in the age calculation; nt—total number of crystals analyzed.

#Unit name is newly designated by this study because the unit was previously unnamed.

§Age calculated at New Mexico Institute of Mining and Mineral Resources. All other ages were calculated at Oregon State University. See Supplemental Appendix C for $^{40}Ar/^{39}Ar$ ideograms and plateaus and Supplemental Appendix D for detailed sample preparation procedures and analytical methods.

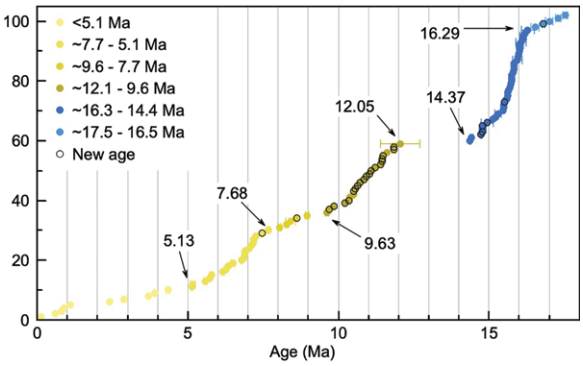

Figure 4. Cumulative age distribution of 102 distinct Miocene regional rhyolite units is shown. All ages are from unique eruptive centers unless ages from multiple units of the same center yielded different ages (not within error of each other). All are $^{40}Ar/^{39}Ar$ ages except for six K-Ar ages from Fiebelkorn et al. (1983) and one radiocarbon age from Robinson and Trimble (1983), all of which are associated with the Newberry Volcano. Ages that represent the beginning and end of a prominent pulse of rhyolitic activity are labeled. Error (2σ) is too small for error bars to show outside of the data point marker for most ages. The three prominent rhyolite episodes occurred at ca. 17.5–14.4 Ma, ca. 12.1–9.6 Ma, and ca. 7.7–5.1 Ma. The mafic pulse at ca. 15–10.1 Ma includes the Owyhee Basalt, Tims Peak Basalt, and units of the Keeney Sequence. See Supplemental Material A.1 (see text footnote 1) for complete list of ages and sources.

plot (Fig. 4) and basic histogram with a 0.5 Ma bin width (Fig. 5), both of which include all existing ages of 102 unique silicic centers in eastern Oregon (Supplemental Material A.1), display a distinct periodicity in rhyolite eruptions with three prominent eruptive episodes between the 17.5 Ma Bald Butte rhyolite and the <1 Ma eruptions associated with the Newberry Volcano.

A probability histogram of these same 102 silicic centers at 2σ using bin widths of 0.3 Ma, 0.5 Ma, and 0.7 Ma and statistical outcome of n = 5000 uniformly distributed data points bolsters the observation of three distinct periods of rhyolitic eruptive activity (Fig. 6). This type of histogram uses the 102 ages and their uncertainties to calculate the probability of an age falling into a bin if given 5000 randomly distributed data points. These statistical histograms were generated with varying bin widths and n values to determine the robustness of the observed periodicity. Though most ages have an uncertainty of <0.1 Ma, a bin width of 0.5 Ma is preferred, because three ages have uncertainty of ≥0.2 Ma, with one having an uncertainty of ±0.66 Ma (Supplemental Material A.1). Histogram results with different n values (n = 500, 1000, or 5000) display little to no discernable variations (Supplemental Material A.1).

The basic histogram and the cumulative age distributions most significantly point out variations in eruptive frequency over time. Eruptive activity initiated with a relatively gradual onset consisting of five rhyolites in an ~1 m.y. duration and began with the 17.53 ± 0.08 Ma eruption of Bald Butte (Ford et al., 2013). Rhyolitic eruptive activity intensified after eruption of the 16.29 ± 0.21 Ma rhyolite of Beulah Reservoir (Hess, 2014), when 38 eruptions occurred in a ~3.5 m.y. period, ceasing after the 14.37 ± 0.02 Ma eruption of the Strawberry rhyolite (Dvorak, 2021).

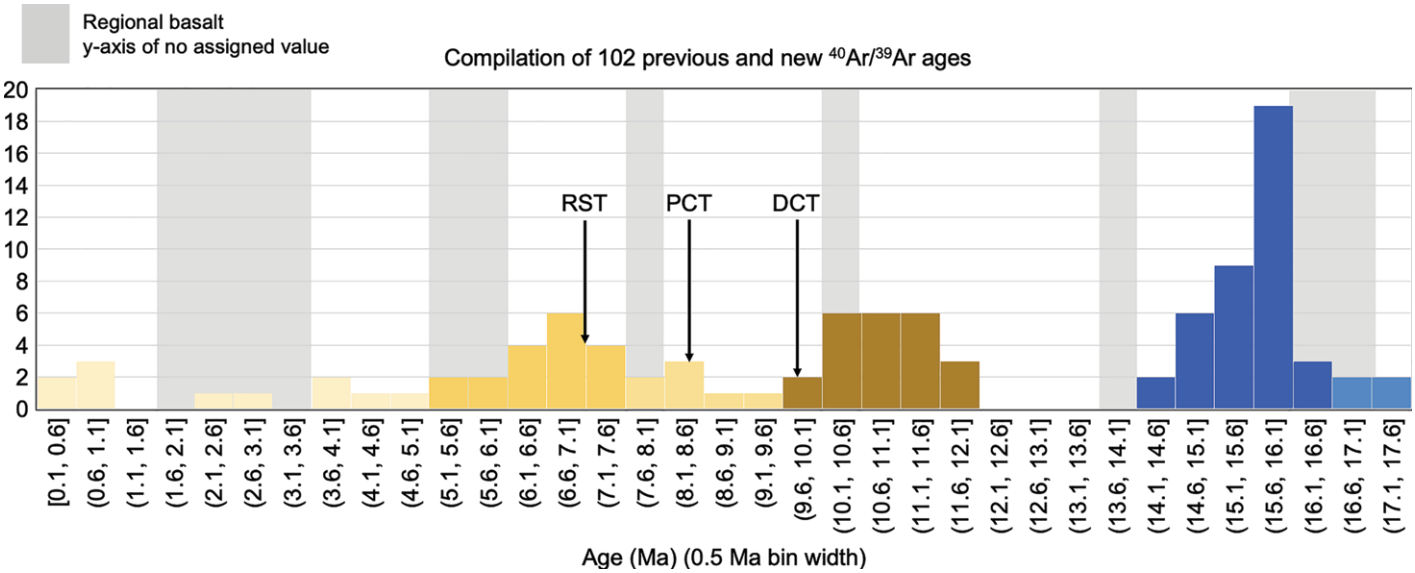

Figure 5. Histogram shows the same 102 ages of unique regional Miocene rhyolites as noted in Figure 4 but using a bin width of 0.5 m.y. Histogram bar colors correspond with those in the cumulative age distribution diagram (Fig. 4). The Rattlesnake Tuff (RST), Prater Creek Tuff (PCT), and Devine Canyon Tuff (DCT) account for more than half of the total volume of rhyolites that erupted in the High Lava Plains (HLP; Ford et al., 2013). Not labeled are the younger and less voluminous 5.1 Ma Potato Lake Tuff and 3.9 Ma Hampton Tuff. The 16.2–15.2 Ma Dinner Creek Tuffs, 15.9 Ma Leslie Gulch Tuff, 15.7 Ma Succor Creek Tuff, 15.5 Ma Wildcat Creek Tuff, and 14.9 Ma Buchanan Tuff of the first eruptive episode are also not labeled. Grey shades represent prominent periods of mafic volcanism (*y*-axis height is of no assigned value); ca. 17.2–16.0 Ma—main phase Columbia River Basalt Group (CRBG) volcanism (e.g., Brueseke et al., 2007; Cahoon et al., 2020); ca. 14.1–13.6 Ma—period of relatively abundant mafic volcanism associated with the Tims Peak Basalt, Owyhee Basalt, and flows of the Keeney Sequence (e.g., Hooper et al., 2002); ca. 10.6–10.0 Ma—period of relatively abundant younger CRBG basalt eruptions and eruptions of the Keeney Sequence (e.g., Barry et al., 2013); 8.0–7.5 Ma, 5.7–5.3 Ma, and 3.0–2.0 Ma—periods of younger mafic volcanism associated with the HLP (e.g., Jordan et al., 2004). These basalt episode ranges have been slightly modified to reflect the complete compilation of ages from additional sources (see Supplemental Material A.2; see text footnote 1).

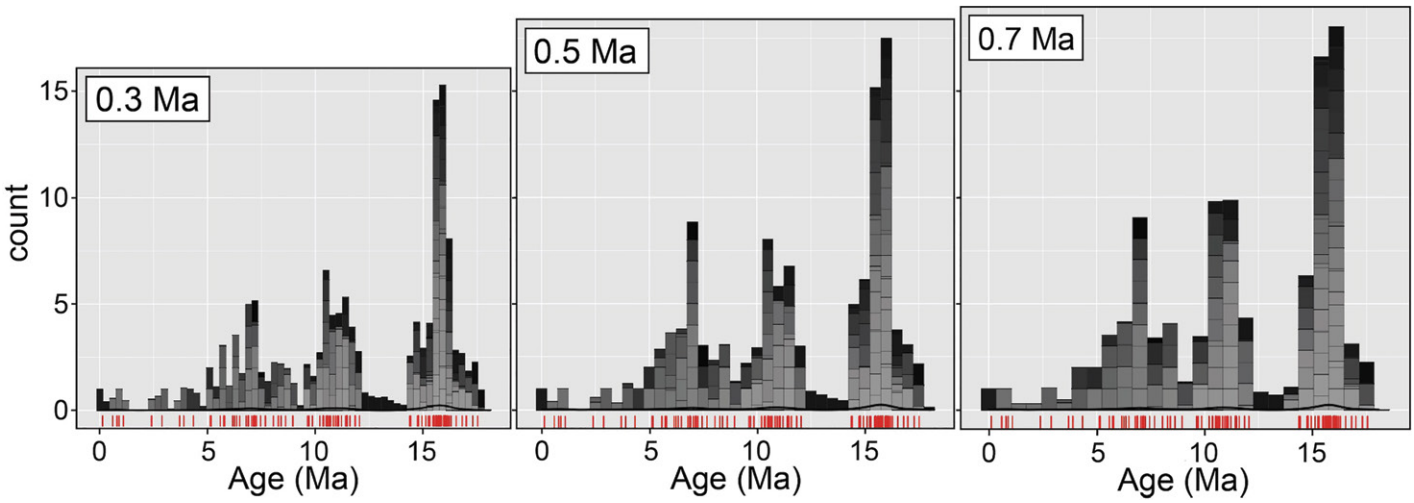

Figure 6. Histograms of regional Miocene rhyolites with 2σ errors using bin widths of 0.3 Ma, 0.5 Ma, and 0.7 Ma were calculated using 1000 uniformly distributed data points. A bin width of 0.5 Ma is preferred, because three ages have uncertainty of ≥0.2 Ma; one has an error of ± 0.66 Ma (Supplemental Material A.1; see text footnote 1). When n values are varied (n = 500, 1000, or 5000), histogram results display little to no discernable variations (Supplemental Material A.1). Density curve using uniformly distributed data points is shown as a solid black line. Each shade of gray represents a unique rhyolite. Red dashes represent actual ages (or mean ages, with respect to the density calculations). Plots were made using R Studio software.

A 2.3 m.y. eruptive hiatus preceded the second prominent 12.1–9.6 Ma episode of 24 rhyolites in a 2.5 m.y. period; it initiated with eruption of the 12.05 ± 0.66 Ma Beatys Butte rhyolite (Scarberry et al., 2010) and concluded after eruptions of the 9.86 ± 0.02 Ma newly defined Griffin Creek rhyolite and the 9.63 ± 0.05 Ma Devine Canyon Tuff (Ford et al., 2013). Only five rhyolite eruptions occurred within the 1.9 m.y. period between eruption of the Devine Canyon Tuff and the 7.68 ± 0.04 Ma rhyolite of Burns Butte (Jordan et al., 2004), which represents a notable waning in rhyolite volcanism at ca. 9.6–7.7 Ma. The third prominent 7.7–5.1 Ma pulse of 20 eruptions in the ~2.6 m.y. period waned after eruption of the 5.13 ± 0.02 Ma Potato Lake Tuff (Sanville, 2015). Ten rhyolite eruptions occurred after 5.1 Ma, starting with eruption of the 4.34 Ma Cougar Mountain rhyolite (Ford et al., 2013) and concluding with the 1.3 ka eruption of Big Obsidian Flow (Robinson and Trimble, 1983). Of these 10 eruptions, seven are associated with Newberry Volcano. It should be noted that the frequency of rhyolite eruptions does not reflect the volume of rhyolite eruptions over time within the HLP. Over half of the volume of rhyolites erupted in the HLP was emplaced between 10 Ma and 7 Ma, which reflects an overall decrease in the volume of rhyolite eruptions through time (e.g., Ford et al., 2013).

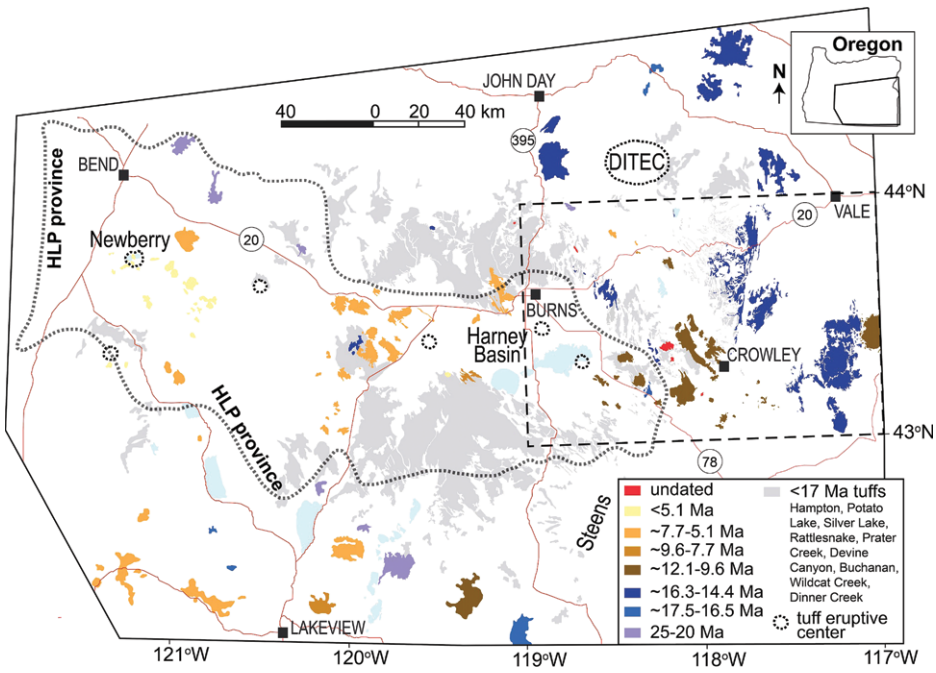

Figure 7. Simplified compilation geologic map shows Miocene rhyolite centers throughout southeastern Oregon. High Lava Plains (HLP) province extent is from Ford et al. (2013). Map sources include Ferns et al. (1993a, 1993b), Greene et al. (1972), Jordan et al. (2004), Jenks et al. (2006, 2007), Ford et al. (2013), Streck et al. (2015), and Webb et al. (2019). See Supplemental Material A.1 for complete list of age sources (see text footnote 1). DITEC—Dinner Creek eruptive center from Streck et al. (2015). Red lines are highways, and Highways 20, 78, and 395 are labeled.

DISCUSSION

A regional map of Miocene rhyolites with new ages from this study agrees with eruptive space-time trends reported by previous workers (e.g., Ford et al., 2013; Fig. 7). Rhyolites that erupted from ca. 17.5–16.3 Ma were dispersed over a wide area and emplaced as far south as around Lakeview, Oregon, and as far north as Unity, Oregon. Silicic units emplaced from ca.

16.3–14.4 Ma are largely concentrated between ~119–117°W and 43–44°N, with the exceptions of the Horsehead Mountain dacite, Little Juniper Mountain dacite, Donnelly Butte rhyolite, and Wagontire Mountain rhyolite, which erupted further west. Rhyolites that erupted at ca. 12.1–9.6 Ma are located within the primary sampling area (119–117°W and 43–44°N) and most highly concentrated within 43°00′–43°30′N, except for the widely dispersed Devine Canyon Tuff and the rhyolite of Beatys Butte that was emplaced ~80 km southwest of the study area. The five rhyolites that erupted between 9.6 Ma and 7.7 Ma are widespread and were emplaced as far southwest as the rhyolite of Drake Peak near Lakeview, Oregon, and as far northeast as the newly defined south of Drewsey rhyolite. All rhyolites that erupted between 7.7 Ma and 5.1 Ma were emplaced within the HLP except for those that occurred south of the HLP extent near Lakeview, Oregon, which formed seven centers that include Bug Butte, Fergason Mountain, Quartz Mountain, Cougar Peak, and the dome east of Lake Abert (Supplemental Material A.1). Drake Peak, Flint Ridge, and the dome east of Lake Abert, Yamsay Mountain, and Hagar Mountain silicic centers are mostly of intermediate composition and were emplaced west of 119°W but ~10–50 km south of the southern extent of the HLP (Fig. 7), which led some researchers to characterize them as part of the Northwest Basin and Range province (e.g., Ford et al., 2013). All post-5.1 Ma rhyolites are concentrated near Newberry Volcano and the Silver Lake Tuff eruptive center in the eastern HLP province, which lies south of Bend, Oregon.

Initiation of co-CRBG Rhyolite Eruptions at ca. 17.5 Ma and the 17.5–14.4 Ma Rhyolitic Eruptive Episode

The mantle source for the CRBG flood basalts still is a topic of debate; hence, we discuss Miocene co-CRBG rhyolite volcanism in the context of mantle upwellings in general, whether induced by extension or by a deep-sourced mantle plume (cf. Hooper et al., 2002; Camp and Wells, 2021). Strong upwelling, ponding, and radial spreading of mantle beneath eastern Oregon resulted in the CRBG flood basalts beginning at ca. 17.23 Ma (Cahoon et al., 2020). The main phase of flood basalt volcanism occurred from ca. 17.0 Ma to 16.0 Ma (e.g., Camp et al., 2003; Camp, 2019) along with co-CRBG rhyolites. There is only a brief ~0.3 m.y. period between the earliest CRBG flood basalts at ca. 17.23 Ma at and initial co-CRBG rhyolite eruptions at ca. 17.53 Ma. On the other hand, main-phase CRBG flood basalt volcanism beginning at ca. 17.0 Ma occurred ~0.7 m.y. prior to peak co-CRBG rhyolite volcanism at ca. 16.29 Ma. In other bimodal flood basalt provinces around the world, basalt eruptions commonly occur shortly (<2 m.y.) before associated rhyolite eruptions because of the residence time, or lag time, necessary to generate eruptible silicic magma reservoirs (e.g., Streck et al., 2015; Townsend et al., 2019). For example, there is an ~1.1 m.y. gap between flood basalts and rhyolites of the Deccan Traps (Sheth and Pande, 2014), and there is an ~1–2 m.y. gap between the onset of mafic and rhyolitic eruptions in the Karoo province (Duncan et al., 1997; Riley et al., 2004). If this is the case, the ~0.3 m.y. lag time to generate co-CRBG rhyolites is comparatively short. Regions of CRBG magma storage are reflected by the locations of co-CRBG rhyolitic eruptive centers (e.g., Streck et al., 2015; Webb et al., 2019). The few and widespread 17.5–16.3 Ma rhyolite eruptions prior to the relatively focused eruptions of peak co-CRBG rhyolite volcanism suggest a greater distribution of basalt intrusions related to "CRBG mantle upwelling" (whether deep- or shallow-sourced) than previously reported at this time, possibly as far west as Drake Peak and Bald Butte. Upwelling mantle material continued to rapidly accumulate beneath the regional lithosphere, producing main-phase CRBG basalt magmas that triggered the generation of large, eruptible volumes of silicic magmas that denote the peak of co-CRBG rhyolite eruptions.

The 14.4–12.1 Ma Rhyolitic Eruptive Hiatus

The 14.4–12.1 Ma gap in the regional rhyolite age progression reflects a hiatus in rhyolitic eruptive activity that correlates to variations observed in regional mafic magmatism during this period (Fig. 5). Jordan et al. (2004) and Camp (2019) are among several researchers who suggest that migration of the North American craton over the plume tail at ca. 15 Ma caused rapid radial spreading of plume material to transition into the narrow, age-progressive rhyolite volcanism of the YSRP track to the east and the initiation of relatively slow westward spreading in areas primarily west of the craton boundary. Decreased mantle flux could explain the scarcity in mafic eruptions that is broadly concurrent with the ca. 14.4–12.1 Ma period of rhyolitic eruptive quiescence (Fig. 5). Lack of ca. 14.4–12.1 Ma rhyolites in the regional geochronologic record as the result of erosion or burial seems less plausible. Some rhyolites may no longer be exposed due to erosion and deposition related to the ca. 17–10 Ma Northwest Basin and Range extensional faulting. However, with a complete regional geochronologic record of exposed rhyolites, such a clear absence of rhyolite eruptions for the ~2.3 m.y. period of ca. 14.4–12.1 Ma seems unlikely to result solely from erosion and burial.

Three distinct mafic to intermediate volcanic units were emplaced in eastern Oregon between ca. 15.0 Ma and ca. 10.1 Ma, and none have been extensively studied: the ca. 15.0–13.1 Ma tholeiitic to calc-alkaline Owyhee Basalt, the ca. 13.9–13.1 Ma tholeiitic Tims Peak Basalt, and the calc-alkaline ca. 13.5–10.1 Ma Keeney Sequence (Table 1). It should be noted that these age ranges come from sparse ages acquired from only a few erupted units (Table 1; Supplemental Material A.2). In addition, precise volumes of the Owyhee Basalt, Tims Peak Basalt, and Keeney Sequence lavas are not known. Based on previous mapping, stratigraphic measurements, and geochemical data from multiple studies (e.g., Ferns and Cummings, 1992; Lees, 1994; Hooper et al., 2002; Camp et al., 2003), the Keeney Sequence, Tims Peak Basalt, and Owyhee Basalt flows erupted within an ~1344 km^2 area between Venator and Juntura, Oregon, and were dispersed along the eastern and western flanks of the Oregon-Idaho graben. If (1) these flows were originally emplaced throughout the aforementioned ~1344 km^2 area and the entire ~3750 km^2 area of the Oregon-Idaho graben (a total of ~5194 km^2), and (2) present day exposures only represent a mere 30% of the originally emplaced lavas due to erosion or burial, then original emplacement would have occurred over an area of ~17,313 km^2 in the ~5 m.y. duration of these mafic eruptions. For comparison, this generous approximation is only ~8% of the total area of >210,000 km^2 emplaced during main-phase CRBG eruptions in a significantly shorter ~1.5 m.y. period (Reidel et al., 2013). Later studies increased estimated erupted volumes and distributions (Cahoon, et al., 2020). These few and relatively small-volume eruptions may be evidence of a decreased rate of mantle input post-15 Ma that was sufficient to result in waning basaltic volcanism and the hiatus of rhyolite eruptions between ca. 14.4 Ma and 12.1 Ma.

Strong Recommencement of Rhyolite Volcanism at 12.1 Ma and the 12.1–9.6 Ma Eruptive Episode

If decreased mantle flux post-15 Ma is responsible for the 14.1–12.1 Ma rhyolitic eruptive hiatus, this implies that the strong recommencement of rhyolite volcanism at ca. 12.1 Ma resulted from a distinct increase in mantle flux that induced significant crustal melting. Thus, a voluminous mafic eruptive episode within ~2 m.y. before 12.1–9.6 Ma rhyolites is also expected. Although the age ranges are not precise, we can approximate that the Owyhee and Tims Peak Basalt erupted ~1–3 m.y. before

ca. 12.1 Ma, and the ca. 13.5–10.1 Ma Keeney Sequence eruptions coincide with the onset of ca. 12.1 Ma rhyolites. The Owyhee, Tims Peak Basalt, and Keeney Sequence basalts are likely involved in the petrogenesis of 12.1–9.0 Ma rhyolites, but there may be other factors involved, which are addressed below.

The lack of more voluminous ca. 13–12 Ma regional basalts could be attributed to hinderance by the regional crust. The voluminous co-CRBG rhyolite eruptions provide insight into the significant amount of crustal melting and silicic magma storage systems that were active between ca. 17.5 Ma and 14.4 Ma. These older, widespread, erupted and non-erupted rhyolite magmas may have prohibited basaltic magmas from ascending through the crust to the surface (e.g., Ford and Grunder, 2011). Seismic data from Chen et al. (2013) show that crustal thicknesses beneath the Owyhee Plateau east of the HLP province (∼45 km) are slightly greater than crustal thicknesses along the HLP track (∼35 km). Crustal thicknesses and viscosities in easternmost Oregon, though west of the craton boundary, may have been great enough to inhibit mafic magmas from ascending to the surface at ca. 13–12 Ma (Townsend et al., 2019).

It should be noted that the lack of more voluminous ca. 13–11 Ma basalts in the regional geologic record may not necessarily demonstrate a lack of such eruptions at this time. Eastern and central Oregon have been subject to erosion via Basin and Range extensional faulting over the past ∼10 m.y. (Scarberry et al., 2010). Despite the Keeney Sequence, Tims Peak Basalt, and Owyhee Basalt being the only mafic lava units known to have erupted between ca. 13 Ma and 11 Ma in the region of interest, other undocumented flows may have eroded or been buried as a result of Basin and Range tectonism. Additionally, there is a notable lack of precise age and geochemical data for some exposed <15 Ma regional basalts, including those around Highway 20 near Black Butte, north of Drewsey, and around Circle Bar (Camp et al., 2003), some of which are unnamed and some of which are postulated to be associated with the ca. 6.91 ± 1.09 Ma Drinkwater Basalt (K-Ar; Greene et al., 1972). A combination of erosion, younger deposition, and particularly the lack of data could bias the regional record of ca. 13–11 Ma basalts.

Waning of Rhyolite Eruptions from ca. 9.9–9.0 Ma and the 9.0–5.1 Ma Episode

The waning in rhyolitic eruptive activity between ca. 9.6 Ma and 9.0 Ma and the subsequent 9.0–5.1 Ma rhyolitic eruptive episode cannot be clearly explained based on previous research. Ford et al. (2013) noted a lack of reported ages among <10 Ma rhyolites of the HLP and Northwest Basin and Range in three >1 m.y. gaps: 9.6–8.4 Ma, 8.2–7.3 Ma, and 5.8–4.34 Ma. The ages compiled conform with the earliest gap and show a waning in eruptive activity from ca. 9.6–9.0 Ma (Figs. 4–6). We find no significant gap between 8.2 Ma and 7.3 Ma, but this is around the apparent transition between the slow onset period (ca. 9.0–7.3 Ma) and the prominent third pulse of rhyolite eruptions that began at ca. 7.3 Ma. When discussing all 102 rhyolitic eruptive centers in southeast Oregon, no eruptive hiatus is observed within the 5.8–4.34 Ma period. Previous studies have produced ages for six rhyolites within that range: Cougar Mountain, the Potato Lake Tuff, Bug Butte (top), North Connelly Hills, "Juniper Ridge, west," and Glass Buttes "A" (Supplemental Material A.1). However, the 5.17 Ma rhyolite of Bug Butte (top) is ∼80 km southwest of the HLP province extent (Fig. 7), which makes it too far away to be included when discussing the HLP trend. When excluding Bug Butte (top), the 5.13 Ma Potato Lake Tuff is the only rhyolite eruption that occurred within the 1.25 m.y. period between the 5.59 Ma North Connelly Hills rhyolite and the 4.34 Ma Cougar Mountain rhyolite. Thus, 5.6–4.3 Ma is considered a period of waning eruptive activity in both the HLP trend and within all <12 Ma regional rhyolite volcanism.

Of the three episodes of mafic volcanism in the HLP described in previous studies, two coincide with the ca. 9.0–5.1 Ma rhyolites: those that erupted at ca. 8.0–7.5 Ma and those that erupted at 5.9–5.3 Ma (Jordan et al., 2004). Jordan et al. (2004) first noted that the earliest ca. 8.0–7.5 Ma mafic eruptions were soon followed by a pulse of rhyolite volcanism. Our analysis corroborates this finding, with the third eruptive episode initiating at ca. 9.0 Ma and peaking at ca. 7.3 Ma, or ∼0.3 m.y. after the ca. 8.0–7.5 Ma basalts. The ca. 6.91 Ma Drinkwater Basalt (K-Ar; Greene et al., 1972) also erupted during the 9.0–5.1 Ma episode of silicic eruptive activity, and it was emplaced primarily in the area between the Harney Basin and the Oregon-Idaho graben (Camp et al., 2003).

Ford et al. (2013) explained that the waning of basaltic eruptions post-5 Ma likely resulted from decreased basalt flux. Their conclusion coincides with our observed 5.6–4.3 Ma period of lessened rhyolitic eruptive activity as compared to present-day Newberry eruptions. Camp (2019) described the distribution of mantle plume material at this time to be widespread through multiple narrow channels throughout the western HLP, which implies that the heat from the mantle was distributed over a greater extent before eventually pooling against the eastern margin of the Cascade Arc. A combination of decreased mantle volume and heat flux and a higher density crust composed of erupted and non-erupted mafic and silicic melts across millions of years may have hindered younger basalts from ascending through the crust to produce silicic crustal melts (Ford and Grunder, 2011; Ford et al., 2013).

Implications for a Refined Model of High Lava Plains Volcanism

Below, we present evidence for a model to explain <18 Ma rhyolite volcanism of southeast Oregon that focuses on the transition between CRBG- and HLP-age volcanism and the progression of the HLP trend, which is summarized in Table 3.

Nearly all previously proposed models attribute the <12 Ma volcanism of eastern Oregon to westward migration of hotter mantle, and discrepancies between them lie in the source of mantle material and in the force driving the spreading. The primary arguments are for buoyancy-driven spreading of a deep-sourced mantle plume (e.g., Jordan et al., 2004), slab dynamics driving crustal extension and mantle convection (e.g., Ford et al., 2013), or some combination of both (e.g., Kincaid et al., 2013). Regardless of mantle source, models that entail continuous migration or flux of hotter mantle material as the catalyst for crustal melting to produce HLP rhyolites seem less plausible with the newly discovered periodicity in eastern Oregon silicic volcanism, particularly the two prominent pulses after 12.1 Ma. These distinct silicic eruptive episodes demand a model with more punctuated mafic inputs.

The lithosphere in eastern Oregon was left structurally weakened after CRBG magmatism. CRBG magmas resided in the crust in an area south of Baker City to the Oregon-Nevada border and westward to ∼119°W latitude (Camp and Ross, 2004; Wolff et al., 2008), and regions of magma storage are reflected by the occurrence of co-CRBG rhyolites (Streck et al., 2015, 2017; Webb et al., 2019). In other words, the locations of these silicic eruptions correlate with the CRBG basalt storage locations (cf. Wolff et al., 2008). CRBG magmatism was accompanied by significant extension that was expressed as generally north–south-trending faults. Northwest Basin and Range extension apparently began at 17–16 Ma and continued with slightly waning intensity until 12–10 Ma (Colgan and Henry, 2009; Brueseke et al., 2014). CRBG-age extension in areas farther north of the Northwest Basin and Range is evidenced by the north–south-trending feeder dikes of the CRBG flood basalts (Hooper, 1997) and by initiation of the Oregon-Idaho graben at ca. 16 Ma. There is a concentration of relatively unstudied north- to

TABLE 3. SYNOPSIS OF SIGNIFICANT PERIODS IN MIOCENE RHYOLITE ERUPTIVE ACTIVITY AND THE PRIMARY REGIONAL TECTONIC AND MAGMATIC PROCESSES INVOLVED

Timeline of rhyolitic eruptive episodes	Primary mechanisms driving or ceasing rhyolite volcanism
HLP volcanism	
5.1 Ma to present, waning rhyolite volcanism	Sparse rhyolite volcanism is focused in the area around Newberry Volcano in crust influenced by the subduction zone and unaffected by CRBG volcanism.
7.7–5.1 Ma, third major episode of rhyolite volcanism	Onset of eruptive activity coincides with initiation of the Brothers Fault Zone; volcanism occurred within lithosphere less affected by earlier CRBG volcanism.
9.6–7.7 Ma, waning regional eruptive activity	Regional transition between significant north–south Northwest Basin and Range faulting and initiation of the Brothers Fault Zone at ca. 7.5 Ma.
12.1–9.6 Ma, strong recommencement and second major episode of rhyolite volcanism	BFZ normal faulting and shearing, continued NWBR extension and arc rotation, and episodic inputs of melt into the crust facilitated upper mantle-driven HLP volcanism.
14.4–12.1 Ma, prominent hiatus in regional rhyolitic eruptive activity	Mantle flux decreases in the region, which may be a result of the North American plate migrating over the "CRBG mantle upwelling" plume tail.
CRBG volcanism	
16.3–14.4 Ma, first major episode of rhyolite volcanism	Greatest mantle flux and formation of large mafic magma reservoirs; timing of this pulse coincides with voluminous Grande Ronde Basalt volcanism. Co-CRBG extensional faulting is correlated to upwelling of mantle.
17.5–16.5 Ma, gradual onset of co-CRBG rhyolite volcanism	Deep- or shallow-sourced mantle upwelling-induced regional crustal melting and propagation of basaltic magmas through the crust produced rhyolites (either by partial melting or crystal fractionation). Gradual onset reflects basalt magmas ascending unimpeded through the crust prior to major reservoir formation; relatively minimal residence times of mafic magmas within the crust.

Note: BFZ—Brothers Fault Zone; CRBG—Columbia River Basalt Group; HLP—High Lava Plains; NWBR—Northwest Basin and Range.

north-northwest–trending normal faults east of Highway 395, in the area between John Day, Vale, Crowley, and Burns, Oregon. (Figs. 8–9). Previous workers note that these north-striking, near-vertical faults crosscut some co-CRBG rhyolites (Greene et al., 1972; Ferns et al., 1993a, 1993b), which implies that extensional faulting in this locality occurred mainly after and possibly during emplacement of co-CRBG rhyolites. Some of these faults are correlated to the Oregon-Idaho graben, and others have not been studied in enough detail to determine whether they are part of the Northwest Basin and Range extension or due to regional uplift during main phase CRBG magmatism (e.g., Glen and Ponce, 2002), particularly those around the Malheur National Forest in Oregon. In summary, the mantle upwelling that caused CRBG basalt magmatism was the driving force behind the production of co-CRBG rhyolites. Both regional extension and additions of melt into the crust can substantially decrease the strength of the crust (Rosenberg and Handy, 2005; Rosenberg et al., 2007), and these factors impacted the regional lithosphere during CRBG magmatism.

Strong recommencement of rhyolite volcanism at ca. 12.1 Ma reflects a shift in the primary mechanism that drives regional magmatism from this earlier pronounced mantle upwelling as attributed to a deep-sourced plume (e.g., Jordan et al., 2004; Camp, 2019) to regional extensional forces. By this time, the mantle upwelling associated with CRBG volcanism no longer actively affected the area, and this decreased flux of mantle material is evidenced by the 14.4–12.1 Ma hiatus in rhyolite eruptions. Rhyolites of the 12.1–9.6 Ma pulse are mostly concentrated in an area of relatively unstudied north–south-trending normal faults between Burns and Crowley, Oregon, which is within the regional lithosphere impacted by earlier CRBG magmatism (Figs. 7–8). There is evidence for some of these faults crosscutting co-CRBG rhyolites and some crosscutting 12.1–9.6 Ma rhyolites (e.g., Greene et al., 1972), which implies that regional normal faulting occurred during and after both eruptive episodes. Clockwise rotation of Oregon and the Cascade arc has been ongoing since ca. 16 Ma, starting at a rate of ~2 mm/yr, increasing to ~33 mm/yr at ca. 10 Ma, and decreasing to ~5 mm/yr at ca. 5 Ma (Wells and McCaffrey, 2013). Notably, Wells and McCaffrey (2013) mention that they do not have mid-stage data (e.g., 16–10 Ma) to calculate continuous variations in rotation rates. If rotation actually reached a peak rate at ca. 13–12 Ma, this increase in regional faulting and extension combined with ongoing Northwest Basin and Range extension is a significant factor in the strong recommencement of silicic volcanism at 12.1 Ma. A lithosphere structurally weakened by CRBG volcanism subjected to additional extension and rotation would be further weakened by the addition of mafic melts related to the Tims Peak Basalt, Owyhee Basalt, Keeney Sequence basalts, and Strawberry Basalts and basaltic andesites. Compounding of these factors induced the strong recommencement of rhyolite volcanism at ca. 12.1 Ma.

Waning in rhyolitic eruptive activity between ca. 9.6 Ma and 7.7 Ma reflects a shift in the accommodation of continued regional extension and rotation in lithosphere less impacted by CRBG magmatism. The rate of clockwise rotation begins to decrease after ca. 10 Ma (Wells and McCaffrey, 2013). The five eruptions within the ~2 m.y. period between 9.6 Ma and 7.7 Ma occurred within a widespread region that is outside of the extent most significantly impacted by CRBG flood basalt magmatism, as evidenced by the distribution of co-CRBG rhyolites (Fig. 7). Structural evidence suggests that Brothers Fault Zone extensional and transverse faulting began by at least ca. 7.5 Ma (Jordan, 2005). This ~2 m.y. period of decreased rhyolite volcanism falls within the transition between prominent north–south-trending Northwest Basin and Range faulting and initiation of the Brothers Fault Zone. A decrease in regional faulting of lithosphere less affected by CRBG magmatism would result in a decrease in mantle upwelling to generate basalts and coeval rhyolites at ca. 9.6–7.7 Ma.

Continued clockwise Oregon block rotation and initiation of the Brothers Fault Zone are the primary forces responsible for the 7.7–5.1 Ma rhyolite episode. Initiation of the Brothers Fault Zone coincides with the first episode of mafic volcanism in the HLP at ca. 8.0–7.5 Ma (Jordan et al., 2004) and with the onset of peak rhyolitic eruptive activity at ca. 7.7 Ma (Fig. 5; Table 2). The calculated rate of extension throughout the Brothers Fault Zone over the last ca. 8 Ma (~1%) is too low to suggest decompression melting as a primary mechanism in generating HLP mafic magmatism (Jordan et al., 2004; Jordan, 2005), but mafic vents and fissures align with some of the northwest-striking faults of the Brothers Fault Zone, which implies that lavas erupted along structurally controlled fissures (Trench et al., 2012, 2013). Extensional faulting that allowed injection of mafic magmas into the crust would induce crustal melting and rhyolite volcanism between 7.7 Ma and 5.1 Ma. The average rhyolitic eruptive intensity (eruptions per 1 m.y.) during the 7.7–5.1 Ma episode (~8 eruptions per 1 m.y.) is slightly less than that of the 12.1–9.6 Ma episode (~10 eruptions per 1 m.y.), which is likely because volcanism occurred within regional lithosphere that was relatively less affected by CRBG volcanism.

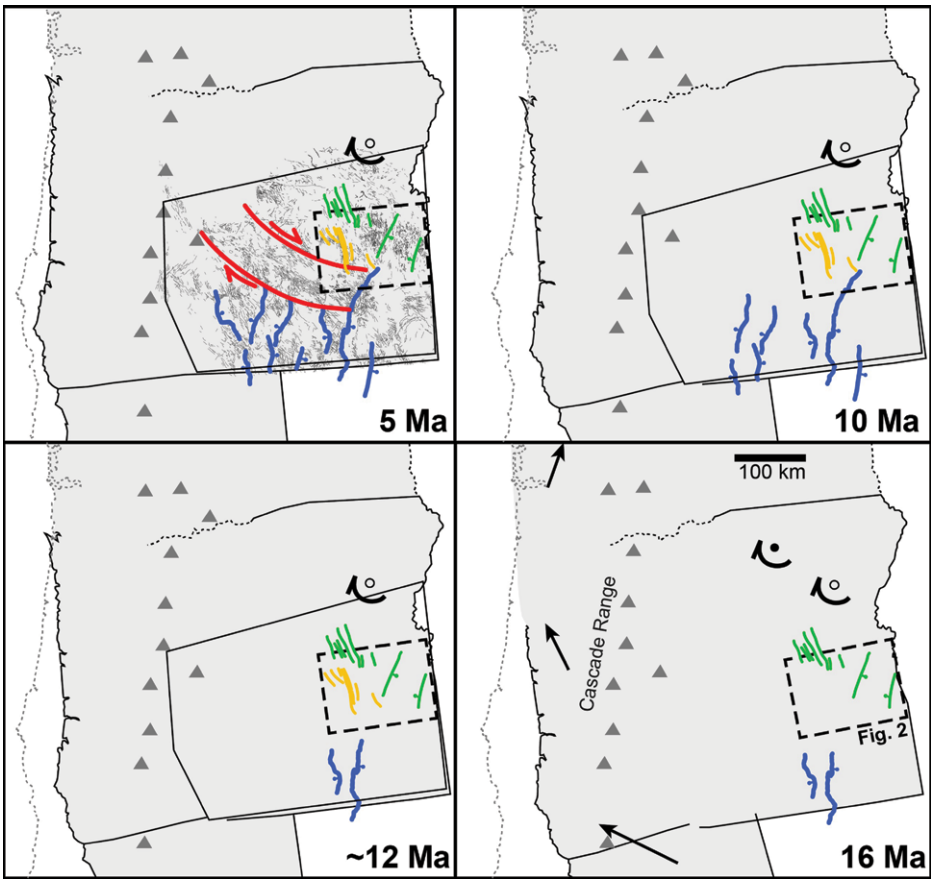

Figure 8. Primary stages of Miocene faulting and Cascade forearc rotation in eastern Oregon are shown. The 16 Ma, 10 Ma, and 5 Ma positions and stages of rotation are from Wells and McCaffrey (2013). The approximate 12 Ma position and stage is inferred from the rotation rate calculated during this time by Wells and McCaffrey (2013). The hollow dot pole of clockwise rotation (preferred) is the approximate pole found perpendicular to tangents of the Brothers Fault Zone envelope, which was calculated by Trench et al. (2013). The solid dot pole of rotation (only shown in 16 Ma panel) is defined by GPS velocities, which were calculated by Wells and McCaffrey (2013). Black arrows in the 16 Ma panel are velocity vectors calculated by Wells and McCaffrey (2013). The solid black line polygon denotes the extent of the map area shown in Figure 7. Major Northwest Basin and Range faults are colored blue. Timing of these faults comes from various sources compiled by Scarberry et al. (2010), with the oldest of these being "Steens Mountain, south" and Catlow Rim (both at ca. 16 Ma). Co-Columbia River Basalt Group (co-CRBG) extensional faults are in green, including the Oregon-Idaho graben. Continued extension occurring near peak rotation rates (Wells and McCaffrey, 2013) resulted in additional N–S extensional faulting at ca. 12 Ma, which is shown in yellow. By 10 Ma, several additional major Northwest Basin and Range faults have activated as regional extension continues. By 5 Ma, extension and shearing as a result of clockwise forearc rotation has generated the Brothers Fault Zone, which is outlined in red.

Most eruptions within the 7.7–5.1 Ma episode occurred within the HLP in the region between the Harney Basin and Newberry Volcano, but when considering rhyolites within and outside of the HLP province, rhyolites of this episode are much more widely dispersed than those of the 12.1–9.6 Ma episode (Fig. 7). The wide distribution of these rhyolites may reflect the influence of back-arc extensional processes (e.g., Christiansen and McKee, 1978; Smith, 1992) or slab rollback in the spreading of upper mantle material and heat flux throughout the central HLP and regions south–southwest near Lakeview, Oregon (Ford et al., 2013).

Trench et al. (2012, 2013) described the relationship between periodic additions of melt to the crust and the initiation of localized faulting to possibly explain the episodic and widespread nature of HLP mafic volcanism despite the consistent rate of extension throughout the entire Brothers Fault Zone after ca. 8 Ma. This relationship would affect the residence times of mafic melts within the crust, and it may explain why episodes of mafic volcanism do not strongly align with the timing and propagation of rhyolitic eruptive activity within the HLP post-9.0 Ma (Fig. 5). Additions of earlier erupted and non-erupted melts within localized areas throughout the HLP would cause local variations in crust density and in how refractory the crust is. These compositional differences would affect the local abundance of faulting and thus affect basalt transmissibility through the crust. Basalt magmas can quickly propagate through the crust without impediment in areas with significant faulting, and in such cases, it is possible that eruptible volumes of rhyolites would not be generated. Localized compositional variations and subsequent effects on regional faulting would explain why HLP mafic volcanism is widespread and not age-progressive like HLP rhyolites despite consistent rates of extension throughout the Brothers Fault Zone.

The driving mechanisms responsible for the waning of rhyolite volcanism after 5.1 Ma are less defined than those of earlier periods of decreased rhyolitic eruptive activity. Of the 10 total post-5.1 Ma eruptions, seven are associated with Newberry Volcano, and all 10 eruptions occurred in a focused region at and southeast of Newberry Volcano (Fig. 7). Proximity of this region to the Cascade Arc fertilized the crust with volatiles (cf. Rowe et al., 2009), aiding in basalt magmatism and the generation of rhyolite magmas. Overall waning of eruptive activity is likely a result of regional extension and shallow mantle upwelling within lithosphere that has not been impacted by CRBG volcanism. Waning post-5 Ma rhyolite volcanism along the western edge of the HLP includes a burst of rhyolite volcanism within the central Oregon Cascades, where projections of the HLP trend and the faults of the Brothers Fault Zone converge. These rhyolites associated with the Deschutes Formation (e.g., Pitcher et al., 2021) may be mainly due to increased intra-arc rifting (e.g., Conrey et al., 2002), yet a detailed analysis of this is beyond the topic of this contribution.

CONCLUSIONS

New ages from this study, combined with the compilation of existing ages, indicate that Miocene rhyolite volcanism of eastern Oregon occurred in three prominent pulses rather than two as previously reported. Co-CRBG rhyolite volcanism initiated gradually at ca. 17.5 Ma, and peak eruptions occurred at ca. 16.3–14.4 Ma. We confirm and refine the subsequent eruptive hiatus to ca. 14.1–12.5 Ma noted in previous studies.

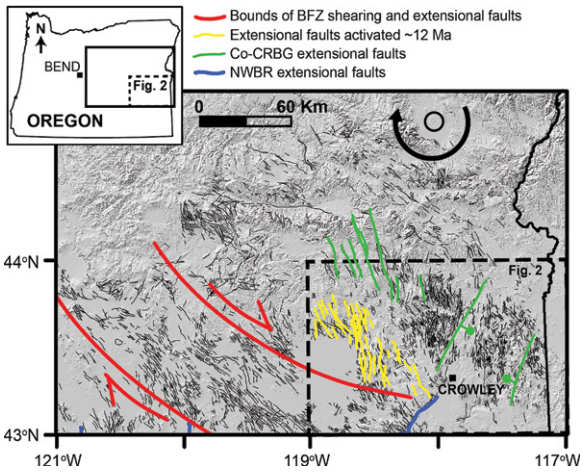

Figure 9. Hillshade map shows eastern Oregon, highlighting areas affected by co-Columbia River Basalt Group (co-CRBG) extensional faults, which are near N–S extensional faults that are proposed to have been activated at ca. 12 Ma, and the bounds of Brothers Fault Zone shearing and extension that initiated by at least 7.5 Ma. All regional faults are noted as thin black lines. Some prominent faults of a particular regime are in bold and colored with respect to their associated tectonic regime. The pole of clockwise rotation (hollow dot) was calculated by Trench et al. (2013). NWBR—Northwest Basin and Range.

A second previously unrecognized episode of rhyolite eruptions occurred at ca. 12.1–9.6 Ma. Rhyolite volcanism waned from ca. 9.6–7.7 Ma. The third eruptive episode occurred at ca. 7.7–5.1 Ma and was followed by decreased rhyolitic eruptive activity that continues at present-day Newberry Volcano.

Rhyolitic eruptive episodes are correlated to (1) the timing of mantle upwelling, basalt generation, and coeval basaltic eruptions and (2) contemporaneous regional tectonic activity. The large influx of mantle plume material in eastern Oregon and the associated CRBG flood basalts provided heat to the crust to induce abundant coeval regional rhyolite volcanism from ca. 16.3–14.1 Ma. The 14.4–12.1 Ma hiatus in rhyolitic eruptive activity reflects a decreased flux of mantle material, as the mantle upwelling associated with CRBG volcanism is no longer actively affecting the area. Rhyolite volcanism of the second (12.1–9.3 Ma) episode is concentrated in the area where the eastern HLP and co-CRBG rhyolites overlap. Strong recommencement of rhyolite volcanism at ca. 12.1 Ma is a result of regional crust weakened by CRBG volcanism experiencing continued Northwest Basin and Range extension and peak clockwise arc rotation rates. Waning of rhyolitic eruptive activity between 9.6 Ma and 7.7 Ma reflects a regional transition between significant north–south Northwest Basin and Range faulting and initiation of the Brothers Fault Zone at ca. 7.5 Ma. The third pulse of rhyolitic eruptive activity (7.7–5.1 Ma) coincides with initiation of the Brothers Fault Zone and occurred within lithosphere less affected by earlier CRBG volcanism. After ca. 5.1 Ma, rhyolite volcanism occurred in a focused area around Newberry Volcano in crust influenced by the subduction zone and unaffected by CRBG volcanism.

This study highlights the magmatic and tectonic complexities involved in continental flood basalt and bimodal volcanic systems. Our interpretations underscore the relationship between faulting and magma storage that can be applied to other global bimodal systems, particularly those influenced by multiple tectonic regimes.

ACKNOWLEDGMENTS

This work was supported through National Science Foundation grant EAR-1220676 to M.J. Streck; and the Geological Society of America and internal Portland State University graduate student research grants to V.M. Swenton. We thank Mark Ford, an anonymous reviewer, and the associate editor for their constructive and detailed reviews. Special thanks to Anita Grunder for discussions and Emily Cahoon for help with R Studio script for statistical analysis. M.J. Streck thanks Mark Ferns for his long-term field collaboration in elucidating eastern Oregon geology.

REFERENCES CITED

Arakawa, Y., Endo, D., Oshika, J., Shinmura, T., and Ikehata, K., 2019, High-silica rhyolites of Niijima Volcano in the northern Izu–Bonin arc, Japan: Petrological and geochemical constraints on magma generation and supply: Lithos, v. 330–331, p. 223–237, https://doi.org/10.1016/j.lithos.2019.02.014.

Barry, T.L., Kelley, S.P., Reidel, S.P., Camp, V.E., Self, S., Jarboe, N.A., Duncan, R.A., and Renne, P.R., 2013, Eruption chronology of the Columbia River Basalt Group *in* Reidel, S.P., Camp, V.E., Ross, M.E., Wolff, J.A., Martin, B.S., Tolan, T.L., and Wells, R.E., eds., The Columbia River Flood Basalt Province: Geological Society of America Special Paper 497, p. 45–66, https://doi.org/10.1130/2013.2497(02).

Bartels, K., Kinzler, R., and Grove, T., 1991, High-pressure phase-relations of primitive high-alumina basalts from Medicine Lake Volcano, Northern California: Contributions to Mineralogy and Petrology, v. 108, p. 253–270, https://doi.org/10.1007/BF00285935.

Benson, T.R., and Mahood, G.A., 2016, Geology of the Mid-Miocene Rooster Comb Caldera and Lake Owyhee Volcanic Field, eastern Oregon: Silicic volcanism associated with Grande Ronde flood basalt: Journal of Volcanology and Geothermal Research, v. 309, p. 96–117, https://doi.org/10.1016/j.jvolgeores.2015.11.011.

Brueseke, M.E., and Hart, W.K., 2008, Geology and petrology of the mid-Miocene Santa Rosa-Calico volcanic field, northern Nevada: Nevada Bureau of Mines and Geology Bulletin 133, 46 p.

Brueseke, M.E., Heizler, M.T., Hart, W.K., and Mertzman, S.A., 2007, Distribution and geochronology of Oregon Plateau (USA) flood basalt volcanism: The Steens Basalt revisited: Journal of Volcanology and Geothermal Research, v. 161, p. 187–214, https://doi.org/10.1016/j.jvolgeores.2006.12.004.

Brueseke, M.E., Callicoat, J.S., Hames, W., and Larson, P.B., 2014, Mid-Miocene rhyolite volcanism in northeastern Nevada: The Jarbidge rhyolite and its relationship to the Cenozoic evolution of the northern Great Basin (USA): Geological Society of America Bulletin, v. 126, p. 1047–1067, https://doi.org/10.1130/B30736.1.

Bryan, S.E., Riley, T.R., Jerram, D.A., Stephens, C.J., and Leat, P.T., 2002, Silicic volcanism: An undervalued component of large igneous provinces and volcanic rift margins, *in* Menzies, M.A., Klemperer, S.L., Ebinger, C.J., and Baker, J., eds., Volcanic Rifted Margins: Geological Society of America Special Paper 362, p. 99–120, https://doi.org/10.1130/0-8137-2362-0.97.

Cahoon, E.B., Streck, M.J., Koppers, A.A.P., and Miggins, D.P., 2020, Reshuffling the Columbia River Basalt chronology—Picture Gorge Basalt, the earliest- and longest-erupting formation: Geology, v. 48, p. 348–352, https://doi.org/10.1130/G47122.1.

Camp, V.E., 1995, Mid-Miocene propagation of the Yellowstone mantle plume head beneath the Columbia River basalt source region: Geology, v. 23, p. 435–438, https://doi.org/10.1130/0091-7613(1995)023<0435:MMPOTY>2.3.CO;2.

Camp, V.E., 2019, Plume-modified mantle flow in the northern Basin and Range and southern Cascadia back-arc region since ca. 12 Ma: Geology, v. 47, p. 695–699, https://doi.org/10.1130/G46144.1.

Camp, V.E., and Ross, M.E., 2004, Mantle dynamics and genesis of mafic magmatism in the intermontane Pacific Northwest: Journal of Geophysical Research: Solid Earth, v. 109, p. 1–14, https://doi.org/10.1029/2003JB002838.

Camp, V.E., and Wells, R.E., 2021, The case for a long-lived and robust Yellowstone hotspot: GSA Today, v. 31, p. 4–10, https://doi.org/10.1130/GSATG477A.1.

Camp, V.E., Ross, M.E., and Hanson, W.E., 2003, Genesis of flood basalts and Basin and Range volcanic rocks from Steens Mountain to the Malheur River Gorge, Oregon: Geological Society of America Bulletin, v. 115, p. 105–128, https://doi.org/10.1130/0016-7606(2003)115<0105:GOFBAB>2.0.CO;2.

Carlson, R.W., and Hart, W.K., 1987, Crustal genesis on the Oregon Plateau: Journal of Geophysical Research: Solid Earth, v. 92, p. 6191–6206, https://doi.org/10.1029/JB092iB07p06191.

Carlson, R.W., and Hart, W.K., 1988, Flood basalt volcanism in the Pacific northwestern United States, *in* Macdougall, J.D., ed., Continental Flood Basalts: Dordrecht, Netherlands, Kluwer Academic Publishers, p. 35–62, https://doi.org/10.1007/978-94-015-7805-9_2.

Chen, C.W., James, D.E., Fouch, M.J., and Wagner, L.S., 2013, Lithospheric structure beneath the High Lava Plains, Oregon, imaged by scattered teleseismic waves: Geochemistry, Geophysics, Geosystems, v. 14, p. 4835–4848, https://doi.org/10.1002/ggge.20284.

Chiesa, S., Civetta, L., De Fino, M., La Volpe, L., and Orsi, G., 1989, The Yemen Trap series: Genesis and evolution of a continental flood basalt province: Journal of Volcanology and Geothermal Research, v. 36, p. 337–350, https://doi.org/10.1016/0377-0273(89)90078-4.

Christiansen, R.L., and McKee, E.H., 1978, Late Cenozoic volcanic and tectonic evolution of the Great Basin and Columbia inter-montane regions, *in* Smith, R.B., and Eaton, G.P., Cenozoic Tectonics and Regional Geophysics of the Western Cordillera: Geological Society of America Memoir 152, p. 283–311, https://doi.org/10.1130/MEM152-p283.

Christiansen, R.L., Foulger, G.R., and Evans, J.R., 2002, Upper-mantle origin of the Yellowstone Hotspot: Geological Society of America Bulletin, v. 114, p. 1245–1256, https://doi.org/10.1130/0016-7606(2002)114<1245:UMOOTY>2.0.CO;2.

Coble, M.A., and Mahood, G.A., 2012, Initial impingement of the Yellowstone plume located by widespread silicic volcanism contemporaneous with Columbia River flood basalts: Geology, v. 40, p. 655–658, https://doi.org/10.1130/G32692.1.

Coble, M.A., and Mahood, G.A., 2016, Geology of the High Rock caldera complex, northwest Nevada, and implications for intense rhyolitic volcanism associated with flood basalt magmatism and the initiation of the Snake River Plain–Yellowstone trend: Geosphere, v. 12, p. 58–113, https://doi.org/10.1130/GES01162.1.

Colgan, J.P., and Henry, C.D., 2009, Rapid middle Miocene collapse of the Mesozoic orogenic plateau in northern-central Nevada: International Geology Review, v. 51, p. 920–961, https://doi.org/10.1080/00206810903056731.

Conrey, R.M., Sherrod, D.R., Hooper, P.R., and Swanson, D.A., 1997, Diverse primitive magmas in the Cascade arc, northwestern Oregon and southern Washington: Canadian Mineralogist, v. 35, p. 367–396.

Conrey, R.M., Taylor, E.M., Donnelly-Nolan, J.M., Sherrod, D.R. and Moore, G.W., 2002, North-central Oregon Cascades: Exploring petrologic and tectonic intimacy in a propagating intra-arc rift, *in* Moore, G.W., ed., Field Guide to Geologic Processes in Cascadia: Oregon Department of Geology and Mineral Industries Special Paper 36, p. 47–90.

Cummings, M.L., Evans, J.G., Ferns, M.L., and Lees, K.R., 2000, Stratigraphic and structural evolution of the middle Miocene synvolcanic Oregon-Idaho graben: Geological Society of America Bulletin, v. 112, p. 668–682, https://doi.org/10.1130/0016-7606(2000)112<668:SASEOT>2.0.CO;2.

Draper, D.S., 1991, Late Cenozoic bimodal magmatism in the northern Basin and Range province of southeastern Oregon: Journal of Volcanology and Geothermal Research, v. 47, p. 299–328, https://doi.org/10.1016/0377-0273(91)90006-L.

Duncan, R.A., Hooper, P.R., Rehacek, J., Marsh, J.S., and Duncan, A.R., 1997, The timing and duration of the Karoo igneous event, southern Gondwana: Journal of Geophysical Research: Solid Earth, v. 102, p. 18,127–18,138, https://doi.org/10.1029/97JB00972.

Dvorak, C.L., 2021, Distribution and characterization of rhyolites of the Strawberry Mountain Volcanics—Evolution of a major rhyolite field associated with Columbia River Basalt Group magmatism, eastern Oregon, USA [M.S. thesis]: Portland, Oregon, Portland State University, 195 p., https://doi.org/10.15760/etd.7726.

Ferns, M.L., and Cummings, M.L., 1992, Geology and mineral resources map of The Elbow Quadrangle, Malheur County, Oregon: Oregon Department of Geology and Mineral Industries Geologic Map Series GMS-62, scale 1:24,000.

Ferns, M.L., Evans, J.G., and Cummings, M.L., 1993a, Geologic map of the Mahogany Mountain 30 × 60 minute quadrangle, Malheur County, Oregon, and Owyhee County, Idaho: Department of Geology and Mineral Industries (DOGAMI) Geological Map GMS-78.

Ferns, M.L., Brooks, H.C., Evans, J.G., and Cummings, M.L., 1993b, Geologic map of the Vale 30 × 60 minute quadrangle, Malheur County, Oregon, and Owyhee County, Idaho: Department of Geology and Mineral Industries (DOGAMI) Geological Map GMS-77.

Fiebelkorn, R.B., Walker, G.W., MacLeod, N.S., McKee, W.H., and Smith, J.G., 1983, Index to K-Ar determinations for the state of Oregon: Isochron/West, v. 37, p. 4–60.

Ford, M.T., and Grunder, A.L., 2011, Compositional trends in High Lava Plains and Northwest Basin and Range rhyolites, comparisons to Snake River Plain, Cascades and Iceland: Partial melt, fractionation, or both?: Geological Society of America Abstracts with Programs, v. 43, no. 4, p. 5.

Ford, M.T., Grunder, A.L., and Duncan, R.A., 2013, Bimodal volcanism of the High Lava Plains and Northwestern Basin and Range of Oregon: Distribution and tectonic implications of age-progressive rhyolites: Geochemistry, Geophysics, Geosystems, v. 14, p. 2836–2857, https://doi.org/10.1002/ggge.20175.

Glen, J.M.G., and Ponce, D.A., 2002, Large-scale fractures related to inception of the Yellowstone hotspot: Geology, v. 30, p. 647–650, https://doi.org/10.1130/0091-7613(2002)030<0647:LSFRTI>2.0.CO;2.

Greene, R.C., Walker, G.W., and Corcoran, R.E., 1972, Geologic map of the Burns quadrangle, Oregon: U.S. Geological Survey Miscellaneous Investigations Map I-680, scale 1:250,000, 1 sheet, 1 p. text.

Griffiths, R.W., and Campbell, I.H., 1991, On the dynamics of long-lived plume conduits in the convecting mantle: Earth and Planetary Science Letters, v. 103, p. 214–227, https://doi.org/10.1016/0012-821X(91)90162-B.

Hart, W.K., Aronson, J.L., and Mertzman, S.A., 1984, Areal distribution and age of low-K, high alumina olivine tholeiitic magmatism in the northwestern Great Basin: Geological Society of America Bulletin, v. 95, p. 185–195, https://doi.org/10.1130/0016-7606(1984)95<186:ADAAOL>2.0.CO;2.

Hawley, W.B., and Allen, R.M., 2019, The fragmented death of the Farallon Plate: Geophysical Research Letters, v. 46, p. 7386–7394, https://doi.org/10.1029/2019GL083437.

Hess, E.N., 2014, Strontium, lead, and oxygen isotopic signatures of mid-Miocene silicic volcanism in eastern Oregon [M.S. thesis]: Portland, Oregon, Portland State University, 102 p., https://doi.org/10.15760/etd.2077.

Hooper, P.R., 1997, The Columbia River flood basalt province: Current status, in large igneous provinces: Continental, oceanic, and planetary flood volcanism: Washington, D.C., American Geophysical Union, Geophysical Monograph Series, v. 100, p. 1–27, https://doi.org/10.1029/GM100p0001.

Hooper, P.R., and Hawkesworth, C.J., 1993, Isotopic and geochemical constraints on the origin and evolution of the Columbia River Basalt: Journal of Petrology, v. 34, p. 1203–1246, https://doi.org/10.1093/petrology/34.6.1203.

Hooper, P.R., Binger, G.B., and Lees, K.R., 2002, Ages of the Steens and Columbia River flood basalts and their relationship to extension-related calc-alkalic volcanism in eastern Oregon: Geological Society of America Bulletin, v. 114, p. 43–50, https://doi.org/10.1130/0016-7606(2002)114<0043:AOTSAC>2.0.CO;2.

Jenks, M.D., Ferns, M.L., Staub, P.E., Madin, I.P., Geitgey, R.P., Ma, L., and Niewendorp, C.A., 2006, Oregon statewide geologic map data: Preliminary geologic compilation map of the southeast portion of Oregon: Oregon Department of Geology and Mineral Industries (DOGAMI) Open-File Report O-06-04, scale 1:100,000.

Jenks, M.D., Mertzman, S.A., Wiley, T.J., Staub, P.E., Drazba, M., Ma, L., Niewendorp, C.A., and Madin, I.P., 2007, Preliminary geologic compilation map of the southwest portion of Oregon: Oregon Department of Geology and Mineral Industries (DOGAMI) Open-File Report O-07-16, scale 1:100,000.

Johnson, J.A., and Grunder, A.L., 2000, The making of intermediate composition magma in a bimodal suite: Duck Butte Eruptive Center, Oregon, USA: Journal of Volcanology and Geothermal Research, v. 95, p. 175–195, https://doi.org/10.1016/S0377-0273(99)00125-0.

Jordan, B.T., 2002, Basaltic volcanism and tectonics of the High Lava Plains, southeastern Oregon [Ph.D. dissertation]: Corvallis, Oregon State University, 235 p.

Jordan, B.T., 2005, Age-progressive volcanism of the Oregon High Lava Plains: Overview and evaluation of tectonic models *in* Foulger, G.R., Natland, J.H., Presnall, D.C., and Anderson, D.L., eds., Plates, Plumes and Paradigms: Geological Society of American Special Paper 388, p. 1–22, https://doi.org/10.1130/0-8137-2388-4.503.

Jordan, B.T., Grunder, A.L., Duncan, R.A., and Deino, A.L., 2004, Geochronology of age-progressive volcanism of the Oregon High Lava Plains: Implications for the plume interpretation of Yellowstone: Journal of Geophysical Research: Solid Earth, v. 109, p. 1–19, https://doi.org/10.1029/2003JB002776.

Kincaid, C., Druken, K.A., Griffiths, R.W., and Stegman, D.R., 2013, Bifurcation of the Yellowstone plume driven by subduction-induced mantle flow: Nature Geoscience, v. 6, p. 395–399, https://doi.org/10.1038/ngeo1774.

Leeman, W., and Streck, M.J., 2021, Late Cenozoic magmatism of the northwestern U.S.—The role of sub-continental lithospheric mantle (SCLM): Geological Society of America Abstracts with Programs, v. 53, no. 6, https://doi.org/10.1130/abs/2021AM-368728.

Lees, K.R., 1994, Magmatic and tectonic changes through time in the Neogene volcanic rocks of the Vale area, Oregon, northwestern USA [Ph.D. dissertation]: Milton Keynes, UK, Open University, 284 p.

Linneman, S.R., and Myers, J.D., 1990, Magmatic inclusions in the Holocene rhyolites of Newberry Volcano, central Oregon: Journal of Geophysical Research: Solid Earth, v. 95, p. 17,677–17,691, https://doi.org/10.1029/JB095iB11p17677.

Long, M.D., Gao, H., Klaus, A., Wagner, L.S., Fouch, M.J., James, D.E., and Humphreys, E., 2009, Shear wave splitting and the pattern of mantle flow beneath eastern Oregon: Earth and Planetary Science Letters, v. 288, p. 359–369, https://doi.org/10.1016/j.epsl.2009.09.039.

Lowry, A.R., Ribe, N.M., and Smith, R.B., 2000, Dynamic elevation of the Cordillera, western United States: Journal of Geophysical Research. Solid Earth, v. 105, p. 23371–23390, https://doi.org/10.1029/2000JB900182.

MacLean, J.W., 1994, Geology and geochemistry of Juniper Ridge, Horsehead Mountain and Burns Butte: Implications for the petrogenesis of silicic magma on the High Lava Plains, southeastern Oregon [M.S. thesis]: Corvallis, Oregon State University, 153 p.

MacLeod, N.S., Walker, G.W., and McKee, E.H., 1976, Geothermal significance of eastward increase in age of upper Cenozoic rhyolitic domes in southeastern Oregon: Proceedings, Second United Nations Symposium on the Development and Use of Geothermal Resources, San Francisco, California, v. 1, p. 465–474.

McKee, E.H., and Walker, G.W., 1976, Potassium-argon ages of late Cenozoic silicic volcanic rocks, southeastern Oregon: Isochron/West, v. 15, p. 37–41.

Morgan, W.J., 1981, Hotspot tracks and the opening of the Atlantic and Indian Oceans, *in* Emiliani, C., ed., The Oceanic Lithosphere: New York, John Wiley, p. 443–487.

Parsons, T., Thompson, G.S., and Sleep, N.H., 1994, Mantle plume influence on the Neogene uplift and extension of the U.S. western Cordillera: Geology, v. 22, p. 83–86, https://doi.org/10.1130/0091-7613(1994)022<0083:MPIOTN>2.3.CO;2.

Perkins, M.E., and Nash, B.P., 2002, Explosive silicic volcanism of the Yellowstone hotspot: The ash fall tuff record: Geological Society of America Bulletin, v. 114, p. 367–381, https://doi.org/10.1130/0016-7606(2002)114<0367:ESVOTY>2.0.CO;2.

Pierce, K.L., and Morgan, L.A., 1992, The track of the Yellowstone hot spot: Volcanism, faulting, and uplift, *in* Link, P.K., et al., eds., Regional Geology of Eastern Idaho and Western Wyoming: Geological Society of America Memoir, v. 179, p. 1–53, https://doi.org/10.1130/MEM179-p1.

Pierce, K.L., Morgan, L.A., and Saltus, R.W., 2000, Yellowstone plume head: Postulated tectonic relations to the Vancouver slab, continental boundaries, and climate: U.S. Geological Survey Open File Report 00-498, 39 p.

Pitcher, B.W., Kent, A.J., and Grunder, A.L., 2021, Tephrochronology of North America's most recent arc-sourced ignimbrite flare-up: The Deschutes Formation of the Central Oregon Cascades: Journal of Volcanology and Geothermal Research, v. 412, p. 1–23, https://doi.org/10.1016/j.jvolgeores.2021.107193.

Reidel, S.P., Camp, V.E., Tolan, T.L., and Martin, B.S., 2013, The Columbia River flood basalt province: Stratigraphy, areal extent, volume, and physical volcanology, *in* Reidel, S.P., Camp, V.E., Ross, M.E., Wolff, J.A., Martin, B.S., Tolan, T.L, and Wells, R.E., eds., The Columbia River Flood Basalt Province: Geological Society of America Special Paper 497, p. 1–43, https://doi.org/10.1130/2013.2497(01).

Riley, T.R., Millar, I.L., Watkeys, M.K., Curtis, M.L., Leat, P.T., Klausen, M.B., and Fanning, C.M., 2004, U-Pb zircon (SHRIMP) ages for the Lebombo rhyolites, South Africa: Refining the duration of Karoo volcanism: Journal of the Geological Society, v. 161, p. 547–550, https://doi.org/10.1144/0016-764903-181.

Robinson, S.W., and Trimble, D.A., 1983, U.S. Geological Survey, Menlo Park, California, radiocarbon measurements III: Radiocarbon, v. 25, p. 143–151, https://doi.org/10.1017/S0033822200005336.

Rosenberg, C.L., and Handy, M.R., 2005, Experimental deformation of partially melted granite revisited: Implications for the continental crust: Journal of Metamorphic Geology, v. 23, p. 19–28, https://doi.org/10.1111/j.1525-1314.2005.00555.x.

Rosenberg, C.L., Medvedev, S., and Handy, M.R., 2007, Effects of melting on faulting and continental deformation, *in* Handy, M.R., Hirth, G., and Hovius, N., eds., Tectonic Faults: Agents of Change on a Dynamic Earth: Cambridge, Massachusetts, MIT Press, p. 357–402.

Rowe, M.C., Kent, A.J., and Nielsen, R.L., 2009, Subduction influence on oxygen fugacity and trace and volatile elements in basalts across the Cascade volcanic arc: Journal of Petrology, v. 50, p. 61–91, https://doi.org/10.1093/petrology/egn072.

Sales, H.J., 2018, The Wildcat Creek Tuff, eastern Oregon: Co-eruption of crystal-poor rhyolite and Fe-rich andesite with implication for mafic underpinnings to voluminous A-type rhyolites [M.S. thesis]: Portland, Oregon, Portland State University, 151 p., https://doi.org/10.15760/etd.6245.

Sanville, H.J., 2015, The Hampton Tuff, High Lava Plains, Oregon: Implications for westward migrating silicic volcanism [M.S. thesis]: Corvallis, Oregon, Oregon State University, 143 p.

Scarberry, K.C., Meigs, A.J., and Grunder, A.L., 2010, Faulting in a propagating continental rift: Insight from the late Miocene structural development of the Abert Rim fault, southern Oregon, USA: Tectonophysics, v. 488, p. 71–86, https://doi.org/10.1016/j.tecto.2009.09.025.

Shervais, J.W., and Hanan, B.B., 2008, Lithospheric topography, tilted plumes, and the track of the Snake River–Yellowstone hot spot: Tectonics, v. 27, TC5004, https://doi.org/10.1029/2007TC002181.

Sheth, H.C., and Pande, K., 2014, Geological and $^{40}Ar/^{39}Ar$ age constraints on late-stage Deccan rhyolitic volcanism, inter-volcanic sedimentation, and the Panvel flexure from the Dongri area, Mumbai: Journal of Asian Earth Sciences, v. 84, p. 167–175, https://doi.org/10.1016/j.jseaes.2013.08.003.

Smith, A.D., 1992, Back-arc convection model for Columbia River Basalt genesis: Tectonophysics, v. 207, p. 269–285, https://doi.org/10.1016/0040-1951(92)90390-R.

Smith, R.B., and Braille, L.W., 1994, The Yellowstone hotspot: Journal of Volcanology and Geothermal Research, v. 61, p. 121–188, https://doi.org/10.1016/0377-0273(94)90002-7.

Steiner, A., and Streck, M.J., 2013, The Strawberry Volcanics: Generation of "orogenic" andesites from tholeiite within an intra-continental volcanic suite centered on the Columbia River flood basalt province, USA, *in* Gómez-Tuena, A., Straub, S.M., and Zellmer, G.F., eds., Orogenic Andesites and Crustal Growth: Geological Society, London, Special Publication 385, p. 281–302, https://doi.org/10.1144/SP385.12.

Steiner, A., and Streck, M.J., 2018, Voluminous and compositionally diverse, middle Miocene Strawberry Volcanics of NE Oregon: Magmatism cogenetic with flood basalts of the Columbia River Basalt Group, *in* Poland, M.P., Garcia, M.O., Camp, V.E., and Grunder, A., eds., Field Volcanology: A Tribute to the Distinguished Career of Don Swanson: Geological Society of America Special Paper 538, p. 41–62, https://doi.org/10.1130/2018.2538(03).

Streck, M. J., and Grunder, A. L., 1997, Compositional Gradients and Gaps in High-silica Rhyolites of the Rattlesnake Tuff, Oregon: Journal of Petrology, v. 38, p. 133–163, https://doi.org/10.1093/petroj/38.1.133.

Streck, M.J., and Grunder, A.L., 2008, Phenocryst-poor rhyolites of bimodal, tholeiitic provinces: The Rattlesnake Tuff and implications for mush extraction models: Bulletin of Volcanology, v. 70, p. 385–401, https://doi.org/10.1007/s00445-007-0144-3.

Streck, M.J., and Grunder, A.L., 2012, Temporal and crustal effects on differentiation of tholeiite to calcalkaline and ferro-trachytic suites, High Lava Plains, Oregon, USA: Geochemistry, Geophysics, Geosystems, v. 13, p. 1–23, https://doi.org/10.1029/2012GC004237.

Streck, M.J., Ferns, M.L., and McIntosh, W., 2015, Large, persistent rhyolitic magma reservoirs above Columbia River Basalt storage sites: The Dinner Creek Tuff eruptive center, eastern Oregon: Geosphere, v. 11, p. 226–235, https://doi.org/10.1130/GES01086.1.

Streck, M.J., McIntosh, W.C., and Ferns, M.L., 2017, Columbia River rhyolites: Age-distribution patterns and their implications for arrival, location, and dispersion of flood basalt magmas in the crust: Geological Society of America Abstracts with Programs, v. 49, no. 6, https://doi.org/10.1130/abs/2017AM-302368.

Tian, W., Campbell, I.H., Allen, C.M., Guan, P., Pan, W., Chen, M., Yu, H., and Zhu, W., 2010, The Tarim picrite-basalt-rhyolite suite, a Permian flood basalt from Northwest China with contrasting rhyolites produced by fractional crystallization and anatexis: Contributions to Mineralogy and Petrology, v. 160, p. 407–425, https://doi.org/10.1007/s00410-009-0485-3.

Till, C.B., Grove, T.L., Carlson, R.W., Donnelly-Nolan, J.M., Fouch, M.J., Wagner, L.S., and Hart, W.K., 2013, Depths and temperatures of <10.5 Ma mantle melting and the lithosphere-asthenosphere boundary below southern Oregon and northern California: Geochemistry, Geophysics, Geosystems, v. 14, p. 864–879, https://doi.org/10.1002/ggge.20070.

Townsend, M., Huber, C., Degruyter, W., and Bachmann, O., 2019, Magma chamber growth during intercaldera periods: Insights from thermo-mechanical modeling with applications to Laguna del Maule, Campi Flegrei, Santorini, and Aso: Geochemistry, Geophysics, Geosystems, v. 20, p. 1574–1591, https://doi.org/10.1029/2018GC008103.

Trench, D., Meigs, A., and Grunder, A., 2012, Termination of the northwestern Basin and Range province into a clockwise rotating region of transtension and volcanism, southeast Oregon: Journal of Structural Geology, v. 39, p. 52–65, https://doi.org/10.1016/j.jsg.2012.03.007.

Trench, D., Meigs, A., and Grunder, A., 2013, Corrigendum to "Termination of the northwestern Basin and Range province into a clockwise rotating region of transtension and volcanism, southeast Oregon" [Journal of Structural Geology v. 39, p. 52–65]: Journal of Structural Geology, v. 48, p. 162–163, https://doi.org/10.1016/j.jsg.2012.12.002.

Walker, G.W., 1974, Some implications of late Cenozoic volcanism to geothermal potential in the High Lava Plains of south-central Oregon: Ore Bin, v. 36, p. 109–119, https://doi.org/10.3133/ofr741121.

Walker, G.W., 1979, Revisions to the Cenozoic stratigraphy of Harney Basin, southeastern Oregon: U.S. Geological Survey Bulletin 1475, 41 p.

Webb, B.M., Streck, M.J., McIntosh, W.C., and Ferns, M.L., 2019, The Littlefield rhyolite and associated mafic lavas: Bimodal volcanism of the Columbia River magmatic province, with constraints on age and storage sites of Grande Ronde Basalt magmas: Geosphere, v. 15, p. 60–84, https://doi.org/10.1130/GES01695.1.

Weinberg, R.F., 1997, Rise of starting plumes through mantle of temperature-, pressure-, and stress-dependent viscosity: Journal of Geophysical Research: Solid Earth, v. 102, p. 7613–7623, https://doi.org/10.1029/97JB00266.

Wells, R.E., and McCaffrey, R., 2013, Steady rotation of the Cascade arc: Geology, v. 41, p. 1027–1030, https://doi.org/10.1130/G34514.1.

Wells, R., Bukry, D., Friedman, R., Pyle, D., Duncan, R., Haeussler, P., and Wooden, J., 2014, Geologic history of Siletzia, a large igneous province in the Oregon and Washington Coast Range: Correlation to the geomagnetic polarity time scale and implications for a long-lived Yellowstone hotspot: Geosphere, v. 10, p. 692–719, https://doi.org/10.1130/GES01018.1.

Wright, W.E., Baisan, C., Streck, M., Wright, W.W., and Szejner, P., 2016, Dendrochronology and middle Miocene petrified oak: Modern counterparts and interpretation: Palaeogeography, Palaeoclimatology, Palaeoecology, v. 445, p. 38–49, https://doi.org/10.1016/j.palaeo.2015.12.023.

Wolff, J.A., Ramos, F.C., Hart, G.L., Patterson, J.D., and Brandon, A.D., 2008, Columbia River flood basalts from a centralized crustal magmatic system: Nature Geoscience, v. 1, p. 177–180, https://doi.org/10.1038/ngeo124.

Zhou, Q., Liu, L., and Hu, J., 2018, Western US volcanism due to intruding oceanic mantle driven by ancient Farallon slabs: Nature Geoscience, v. 11, p. 70–76, https://doi.org/10.1038/s41561-017-0035-y.

Science Editor: Brad S. Singer
Associate Editor: Richard Waitt

Manuscript Received 23 September 2021
Revised Manuscript Received 12 May 2022
Manuscript Accepted 22 June 2022

Printed in the USA